21. Charo IF, Myers SJ, Herman A, et al. Molecular cloning and functional expression of two monocyte chemoattractant protein 1 receptors reveals alternative splicing of the carboxyl-terminal tails. *Proc Natl Acad Sci U S A*. 1994;91:2752–2756.
22. Wong LM, Myers SJ, Tsou CL, et al. Organization and differential expression of the human monocyte chemoattractant protein 1 receptor gene. Evidence for the role of the carboxyl-terminal tail in receptor trafficking. *J Biol Chem*. 1997;272:1038–1045.
23. Nakayama EE, Tanaka Y, Nagai Y, et al. A CCR2-V64I polymorphism affects stability of CCR2A isoform. *AIDS*. 2004;18:729–738.
24. Wu L, Paxton WA, Kassam N, et al. CCR5 levels and expression pattern correlate with infectability by macrophage-tropic HIV-1, in vitro. *J Exp Med*. 1997;185:1681–1691.
25. Shioda T, Nakayama EE, Tanaka Y, et al. Naturally occurring deletional mutation in the C-terminal cytoplasmic tail of CCR5 affects surface trafficking of CCR5. *J Virol*. 2001;75:3462–3468.

ARTICLE IN PRESS

Available online at www.sciencedirect.com

ScienceDirect

VIROLOGY

ELSEVIER

Virology xx (2008) xxx–xxx

www.elsevier.com/locate/yviro

Comparison of anti-viral activity of rhesus monkey and cynomolgus monkey TRIM5αs against human immunodeficiency virus type 2 infection

Ken Kono, Haihan Song, Yasuhiro Shingai, Tatsuo Shioda, Emi E. Nakayama *

Department of Viral Infections, Research Institute for Microbial Diseases, Osaka University, 3-1, Yamada-oka, Suita-shi, Osaka 565-0871, Japan

Received 9 November 2007; returned to author for revision 28 November 2007; accepted 17 December 2007

Abstract

Human immunodeficiency virus type 2 (HIV-2) strains vary widely in their ability to grow in Old World monkey (OWM) cells. We previously evaluated several HIV-2 isolates for their sensitivity to cynomolgus monkey (CM) TRIM5α, an anti-HIV factor in OWM cells, and found that viruses carrying proline at the 120th position of the capsid protein were sensitive to CM TRIM5α, whereas those with either alanine or glutamine were resistant. In the study presented here, we tested these HIV-2 isolates for their sensitivity to rhesus monkey (Rh) TRIM5α and found that both CM TRIM5α-sensitive and -resistant viruses were restricted by Rh TRIM5α. The variable region 1 of the SPRY domain of Rh TRIM5α appeared to be the determinant of this difference. Furthermore, a mutagenesis study showed that three amino acid residues TFP at the 339th to 341st positions of Rh TRIM5α are important for restricting HIV-2 strains resistant to CM TRIM5α.

Keywords: TRIM5α; Human immunodeficiency virus; Rhesus monkey; Cynomolgus monkey

Introduction

Human immunodeficiency virus type 1 (HIV-1) has a very narrow host range limited to humans and chimpanzees. Experiments have demonstrated that HIV-1 does not infect Old World monkeys (OWM) such as rhesus and cynomolgus monkeys. Recently, the screening of a rhesus monkey cDNA library identified tripartite motif 5α (TRIM5α) as a factor that confers resistance to HIV-1 infection (Stremlau et al., 2004). Rhesus and cynomolgus monkey TRIM5α restricts HIV-1 infection (Stremlau et al., 2004; Yap et al., 2004; Nakayama et al., 2005), whereas human TRIM5α restricts N-tropic murine leukemia virus (N-MLV) infection (Hatziioannou et al., 2004; Keckesova et al., 2004; Perron et al., 2004). African green monkey (AGM) TRIM5α restricts simian immunodeficiency virus isolated from a macaque monkey (SIVmac), human immunodeficiency virus type 2 (HIV-2), and equine infectious anemia virus in addition to HIV-1 infection (Hatziioannou et al., 2004; Keckesova et al., 2004; Nakayama et al., 2005). TRIM5α shares with other splicing variants a common amino-terminal TRIM motif, comprising RING, B-box and coiled-coil domains, and encodes a unique SPRY (B30.2) domain (Reymond et al., 2001). Several recombinant studies of human and rhesus monkey TRIM5α have shown that the determinant of the species specificity lies in the SPRY domain of TRIM5α (Perez-Caballero et al., 2005; Sawyer et al., 2005; Stremlau et al., 2005; Yap et al., 2005). We also previously demonstrated that 17-amino-acid residues and adjacent AGM-specific 20-amino-acid duplication in the SPRY domain determined species-specific restriction of SIVmac (Nakayama et al., 2005). It is known that the RING and B-box domains are required for restriction and that the coiled-coil domain is required for multimerization (Stremlau et al., 2004; Berthoux et al., 2005; Perez-Caballero et al., 2005; Nakayama et al., 2006). TRIM5α is thought to bind HIV capsid and promote its rapid, premature disassembly in ubiquitin dependent

* Corresponding author. Fax: +81 6 6879 8347.
E-mail address: emien@biken.osaka-u.ac.jp (E.E. Nakayama).

0042-6822/$ - see front matter © 2007 Elsevier Inc. All rights reserved.
doi:10.1016/j.virol.2007.12.022

Please cite this article as: Kono, K., et al., Comparison of anti-viral activity of rhesus monkey and cynomolgus monkey TRIM5αs against human immunodeficiency virus type 2 infection, Virology (2008), doi:10.1016/j.virol.2007.12.022

and independent manners (Stremlau et al., 2006; Diaz-Griffero et al., 2006; Wu et al., 2006; Anderson et al., 2006). This means that the viral RNA and proteins are exposed to cellular proteins and degraded before nuclear transportation.

HIV-2 has a genome extremely similar to that of SIVmac (Hahn et al., 2000). In contrast with the many reports concerning HIV-1 and SIVmac, there have been only a few on susceptibility of HIV-2 to TRIM5α from various species (Nakayama et al., 2005; Ylinen et al., 2005). We previously evaluated eight HIV-2 isolates for their sensitivity to cynomolgus monkey TRIM5α and found that viruses carrying proline at the 119th or 120th position of the capsid protein (CA) were sensitive to cynomolgus monkey TRIM5α, whereas those with either alanine or glutamine were resistant (Song et al., 2007). In the study presented here, we tested these HIV-2 isolates for their sensitivity to another OWM rhesus monkey TRIM5α and found that both cynomolgus monkey TRIM5α-sensitive and -resistant viruses were restricted by rhesus monkey TRIM5α. We were able to show that three amino acid residues TFP at the 339th to 341st positions of rhesus monkey TRIM5α are important for restriction activity against HIV-2 strains.

Results

Rhesus monkey TRIM5α inhibits both cynomolgus monkey TRIM5α-sensitive and -resistant HIV-2 viruses

We previously reported that HIV-2 isolates carrying proline at the 120th position of CA were sensitive to cynomolgus monkey TRIM5α, whereas those with either alanine or glutamine were resistant. Both cynomolgus and rhesus monkey TRIM5αs are known to restrict HIV-1 but not SIVmac. Predicted amino acid sequences of cynomolgus and rhesus monkey TRIM5α are shown in Fig. 1. Rhesus and cynomolgus monkey TRIM5α share 96.8% of amino acid residues. To test these HIV-2 isolates for their sensitivity to rhesus monkey TRIM5α, we constructed a recombinant Sendai virus (SeV) expressing rhesus monkey TRIM5α fused with the HA tag in the C-terminal. Western blot analysis using an antibody against HA-tag showed that rhesus monkey TRIM5α was expressed at similar levels to those of cynomolgus monkey TRIM5α in recombinant SeV infected human T-cell line MT4 cells (data not shown). Fluorescent microscopic observation confirmed that these TRIM5αs were detected in all the cells infected with recombinant SeVs (data not

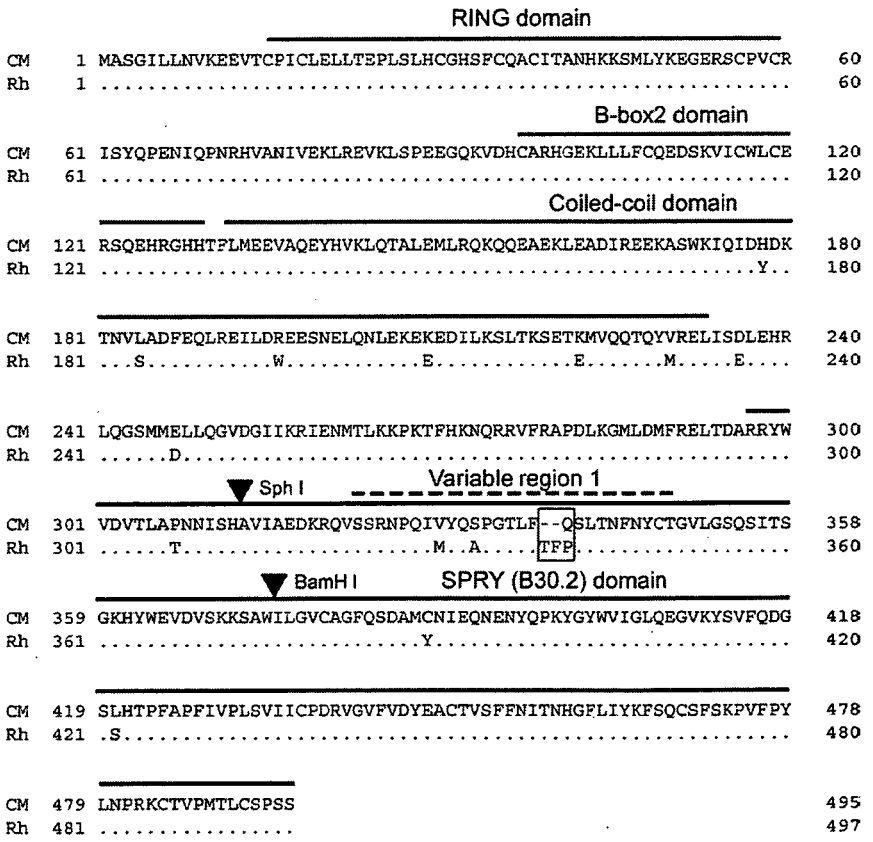

Fig. 1. Alignments of amino acid sequences of cynomolgus monkey (CM) and rhesus monkey (Rh) TRIM5αs. The RING, B-box2, coiled-coil and SPRY (B30.2) domains are indicated by labeled bars over the sequence. Variable region 1 is indicated by a broken bar over the sequence. Dots denote the amino acid residues identical to the one of cynomolgus monkey TRIM5α and dashes a lack of the amino acid residue that is present in rhesus monkey TRIM5α. The box marks amino acid residues that are important for rhesus monkey TRIM5α restriction activity against HIV-2 strains (see Results).

Please cite this article as: Kono, K., et al., Comparison of anti-viral activity of rhesus monkey and cynomolgus monkey TRIM5αs against human immunodeficiency virus type 2 infection, Virology (2008), doi:10.1016/j.virol.2007.12.022

shown). We used SeV expressing cynomolgus monkey TRIM5α lacking the SPRY domain, CM SPRY(−) TRIM5α, as a negative control. MT4 cells infected with recombinant SeV expressing rhesus monkey TRIM5α, cynomolgus monkey TRIM5α, or CM SPRY(−) TRIM5α were then superinfected with an X4-tropic HIV-1 strain NL43, SIVmac239, HIV-2 strain GH123, or GH123/Q which is a mutant HIV-2 carrying glutamine (Q) at the 120th position of CA. In agreement with the results of previous studies, rhesus and cynomolgus monkey TRIM5α could restrict HIV-1 NL43, but failed to restrict SIVmac239 (Fig. 2, upper panels). HIV-2 GH123, cynomolgus monkey TRIM5α-sensitive strain, was restricted by both rhesus and cynomolgus monkey TRIM5αs (Fig. 2, lower left panel), which is also consistent with the findings of previous studies (Song et al., 2007). Despite a high degree of sequence similarity between rhesus and cynomolgus monkey TRIM5αs, rhesus monkey TRIM5α could inhibit replication of HIV-2 GH123/Q, the strain resistant to cynomolgus monkey TRIM5α (Fig. 2, lower right panel).

Variable region 1 (V1) of SPRY (B30.2) domain of rhesus monkey TRIM5α is a determinant for restriction of HIV-2 GH123/Q infection

It is known that the variable region 1 (V1) (Song et al., 2005a,b) of the rhesus monkey TRIM5α SPRY domain is the major determinant of anti-HIV-1 potency (Perez-Caballero et al., 2005; Sawyer et al., 2005; Stremlau et al., 2005; Yap et al., 2005). To determine the precise region of TRIM5α responsible for the anti HIV-2 GH123/Q activity of rhesus monkey TRIM5α, we constructed a recombinant SeV expressing chimeric TRIM5αs between rhesus and cynomolgus monkey TRIM5α by using *Sph*I and *Bam*HI restriction enzyme digestion (Fig. 3A). The central fragment comes from *Sph*I and *Bam*HI digestion contains the V1 of SPRY domain (Fig. 1).

As expected, all forms of chimeric TRIM5α inhibited HIV-1 NL43 and HIV-2 GH123 replication, although the extent of inhibition of HIV-2 GH123 varied among chimeric TRIM5αs (Fig. 3B, left and center panel). On the other hand, 212, 112, and 211 chimeric TRIM5α restricted HIV-2 GH123/Q infection, whereas 121, 221, and 122 chimeric TRIM5α did not (Fig. 3B, right panel), although the expression levels of the latter 1 day after SeV infection were not lower than those of parental and other chimeric TRIM5αs (Fig. 3C). Furthermore, these chimeric TRIM5α expression levels at day 6 after SeV infection were almost equivalent to those at day 1 after SeV infection (data not shown). These results confirmed that stability and kinetics of expression were similar among these chimeric TRIM5αs. Since 212,112, and 211 chimeric TRIM5α possess the rhesus monkey TRIM5α V1, those results indicated that the rhesus monkey TRIM5α V1 is a determinant of anti HIV-2 GH123/Q activity. It is noteworthy that cynomolgus monkey TRIM5α-sensitive HIV-2 GH123 grew to slightly higher titers in the cells

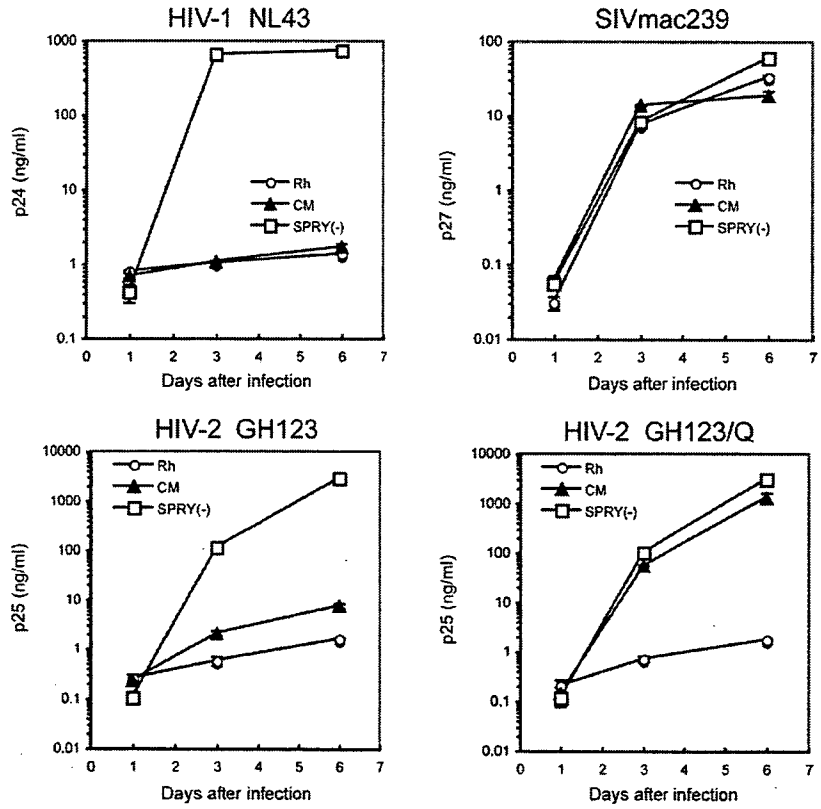

Fig. 2. MT4 cells infected with recombinant SeV expressing rhesus monkey (Rh; O), cynomolgus monkey (CM; ▲), or CM SPRY(−) (□) TRIM5α were inoculated with HIV-1 NL43, SIVmac239, HIV-2 GH123, or HIV-2 GH123/Q. Culture supernatants were respectively assayed for levels of p24, p27, or p25. HIV-2 GH123/Q is a mutant virus carrying glutamine (Q) at the 120th position of HIV-1 GH123 capsid. CM SPRY(−) TRIM5α served as negative control.

Please cite this article as: Kono, K., et al., Comparison of anti-viral activity of rhesus monkey and cynomolgus monkey TRIM5αs against human immunodeficiency virus type 2 infection, Virology (2008), doi:10.1016/j.virol.2007.12.022

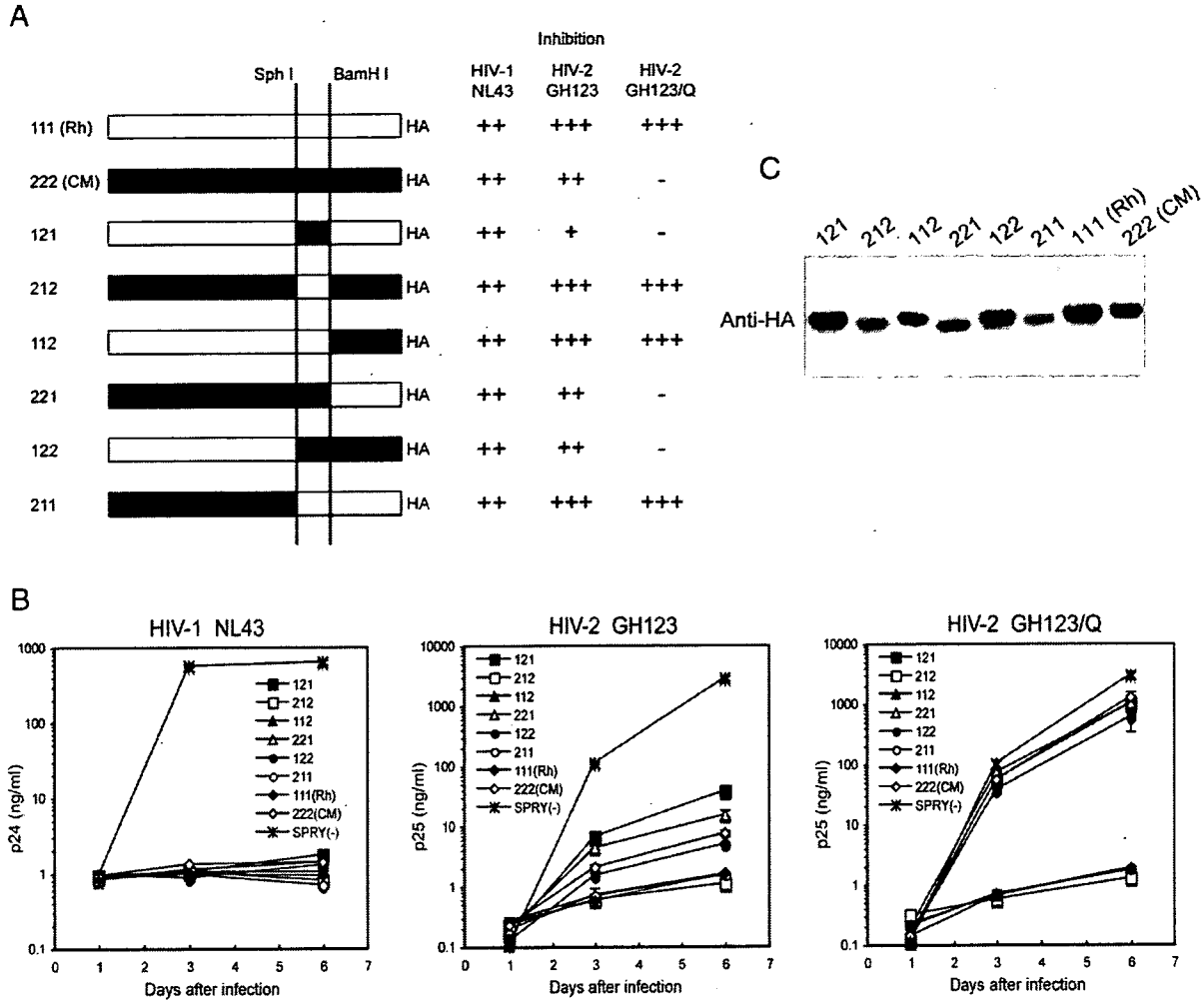

Fig. 3. (A) Schematic representation of chimeric TRIM5αs and summary of the results. White and black bars denote rhesus monkey (Rh) and cynomolgus monkey (CM) sequences, respectively. +++, ++, +, and − denote more than 1000-fold, 100- to 1000-fold, 8- to 100-fold, and less than 8-fold suppression of virus growth, respectively, compared with the negative control on day 6. (B) MT4 cells were infected with recombinant SeV expressing 121 (■), 212 (□), 112 (▲), 221 (△), 122 (●), 211 (○), 111 (Rh) (♦), 222 (CM) (◇), or CM SPRY(−) (*) TRIM5α. Nine hours after infection, cells were inoculated with HIV-1 NL43, HIV-2 GH123, or HIV-2 GH123/Q viruses. Culture supernatants were respectively assayed for levels of p24 or p25. (C) Twenty-four hours after SeV infection, TRIM5α proteins in lysates of MT4 cells infected with recombinant SeV expressing 121, 212, 112, 221, 122, 211, 111 (Rh), or 222 (CM) TRIM5α were visualized by Western blotting with an antibody against HA-tag.

expressing chimeric 121 or 221 TRIM5α than in those expressing parental cynomolgus monkey or 122 chimeric TRIM5α (Fig. 3B, center panel). These results indicate that the extent of inhibition of HIV-2 GH123 by chimeric 121 and 221 TRIM5αs is slightly less than that by parental cynomolgus monkey and 122 chimeric TRIM5α. It has been reported that all three variable regions (V1–V3) could contribute to the anti-viral activity of TRIM5α (Ohkura et al., 2006). It is possible that the combination of the cynomolgus monkey TRIM5α V1 and the rhesus monkey TRIM5α C-terminal portion of the SPRY domain slightly impairs the anti-HIV-2 function of TRIM5α.

V1 of SPRY domain of rhesus monkey TRIM5α is a determinant for broader and more potent anti-HIV-2 activity

To examine the restriction activities of rhesus monkey TRIM5α against other HIV-2 strains, we tested HIV-2 UC2, HIV-2 UC12, and HIV-2 UC14 for their growth potential in human T-cell line Hut78 infected with SeV expressing 121, 212, 111 (rhesus monkey; Rh), 222 (cynomolgus monkey; CM), or SPRY(−) TRIM5α. As shown in Fig. 4, rhesus monkey TRIM5α and cynomolgus monkey chimeric TRIM5α containing the V1 of rhesus monkey TRIM5α (212) completely restricted HIV-2 UC2 and HIV-2 UC14, whereas cynomolgus monkey TRIM5α and rhesus monkey chimeric TRIM5α containing the V1 of cynomolgus monkey TRIM5α (121) failed to do so. Rhesus monkey TRIM5α and 212 chimeric TRIM5α also completely restricted HIV-2 UC12, while cynomolgus monkey TRIM5α did so partially, which is consistent with our previous findings (Song et al., 2007). 121 chimeric TRIM5α showed very weak restriction activity on replication of HIV-2 UC12. Putting these findings together leads us to conclude that the V1 is a determinant for broader and more potent anti-HIV-2 activity of rhesus monkey TRIM5α.

Please cite this article as: Kono, K., et al., Comparison of anti-viral activity of rhesus monkey and cynomolgus monkey TRIM5αs against human immunodeficiency virus type 2 infection, Virology (2008), doi:10.1016/j.virol.2007.12.022

Amino acid residues TFP at the 339th to 341st positions of rhesus monkey TRIM5α are important for inhibiting HIV-2 GH123/Q replication

As shown in Fig. 1, the V1 of the SPRY domain of rhesus monkey TRIM5α contains two amino acid residues TF that are not present in cynomolgus monkey TRIM5α. To examine whether these two additional amino acid residues are responsible for the broad anti-HIV-2 activity of rhesus monkey TRIM5α, we constructed a recombinant SeV expressing rhesus monkey TRIM5α lacking these two amino acid residues (Rh deltaTF TRIM5α). We also constructed a SeV expressing mutant rhesus monkey TRIM5α in which amino acid residues TFP at the 339th to 341st positions were replaced with a single amino acid Q found in cynomolgus monkey TRIM5α (Rh TFP-Q TRIM5α) (Fig. 5A). Expression levels of mutant TRIM5αs in MT4 cells infected with these SeVs were comparable to those of parental TRIM5αs (Fig. 5B).

As shown in Fig. 5C, both of the mutant rhesus monkey TRIM5αs restricted HIV-1 infection. In the case of HIV-2, Rh deltaTF TRIM5α inhibited both HIV-2 GH123 and HIV-2 GH123/Q replications, although anti-HIV-2 activity was slightly weaker than that of parental rhesus monkey TRIM5α. On the other hand, Rh TFP-Q TRIM5α lost its inhibitory activity against HIV-2 GH123/Q, while it could suppress replication of HIV-2 GH123 to the same extent as it was suppressed by 121 chimeric TRIM5α. Conversely, cynomolgus monkey TRIM5α possessing TFP instead of Q at the 339th position (CM Q-TFP TRIM5α) completely restricted HIV-2 GH123/Q replication (Fig. 5D). These results indicated that these three amino acids are important for restricting HIV-2 GH123/Q by rhesus monkey TRIM5α.

Baboon TRIM5α V1 confers anti-viral activity against HIV-2 GH123/Q to cynomolgus monkey TRIM5α, whereas sooty mangabey and pig-tailed monkey TRIM5α V1 fail to do so

HIV-2 is thought to originate from the simian immunodeficiency virus of sooty mangabeys (Hahn et al., 2000). Several HIV-2 isolates could grow in baboon and pig-tailed monkey, and some of them were reported to cause an AIDS-like disease in these animals (Barnett et al., 1994; Locher et al., 1998; Locher et al., 2001; McClure et al., 2000). To assess anti-HIV-2 activity of these OWMs TRIM5αs, we constructed a recombinant SeV expressing cynomolgus monkey chimeric TRIM5α containing the V1 of baboon (2B2), sooty mangabey (2S2), or pig-tailed monkey (2P2) TRIM5α (Fig. 6A). Expression levels of these chimeric TRIM5αs in MT4 cells infected with the SeVs were comparable to those of parental cynomolgus monkey TRIM5α (Fig. 6C). The amino acid sequences of the V1 of baboon, sooty mangabey, and pig-tailed monkey TRIM5α are shown in Fig. 6B. Baboon and sooty mangabey TRIM5α show the SFP sequence at the 339th to 341st positions, whereas pig-tailed monkey TRIM5α has a single Q as cynomolgus monkey TRIM5α. As shown in Fig. 6D, all the chimeric TRIM5αs containing the V1 of baboon, sooty mangabey, and pig-tailed monkey TRIM5α restricted HIV-1 infection. These results are consistent with those of previous studies (Kaiser et al., 2007; Newman et al., 2006; Ohkura et al., 2006). In the case of HIV-2, there were wide variations in anti-HIV-2 activity by the chimeric TRIM5αs. Chimeric TRIM5α containing baboon V1 inhibited both HIV-2 GH123 and HIV-2 GH123/Q replications, while chimeric TRIM5α containing sooty mangabey V1 partially inhibited HIV-2 GH123 and only slightly inhibited HIV-2 GH123/Q replication. Finally, chimeric TRIM5α containing pig-tailed monkey V1 only slightly inhibited both HIV-2 GH123 and HIV-2 GH123/Q replication. This shows that there is a lack of correlation between the effects of various TRIM5αs on HIV-2

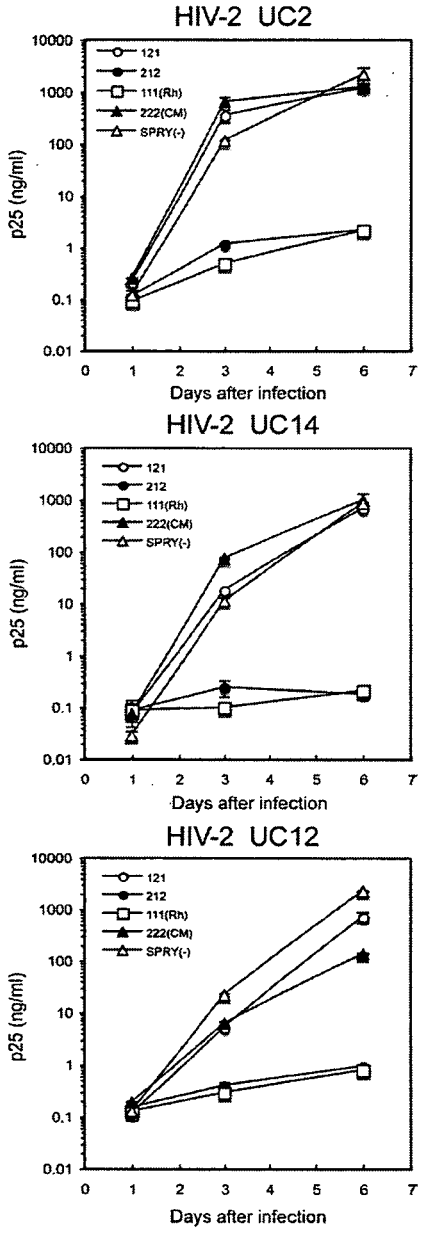

Fig. 4. Hut78 cells infected with recombinant SeV expressing 121 (○), 212 (●), 111 (Rh) (□), 222 (CM) (▲) or CM SPRY(−) (△) TRIM5α. Cells were superinfected with HIV-2 isolates, UC2, UC14, or UC12. Culture supernatants were assayed for levels of p25.

Please cite this article as: Kono, K., et al., Comparison of anti-viral activity of rhesus monkey and cynomolgus monkey TRIM5αs against human immunodeficiency virus type 2 infection, Virology (2008), doi:10.1016/j.virol.2007.12.022

A

	Amino acid sequence	Inhibition HIV-1 NL43	HIV-2 GH123	HIV-2 GH123/Q
Rh	QIMTQAPGTLFTFPSLN	++	+++	+++
CM	..V..S.....--Q...	++	++	-
Rh deltaTF	.....--....	++	++	++
Rh TFP-Q	.....--Q...	++	++	-
CM Q-TFP	..V..S.....	++	+++	+++

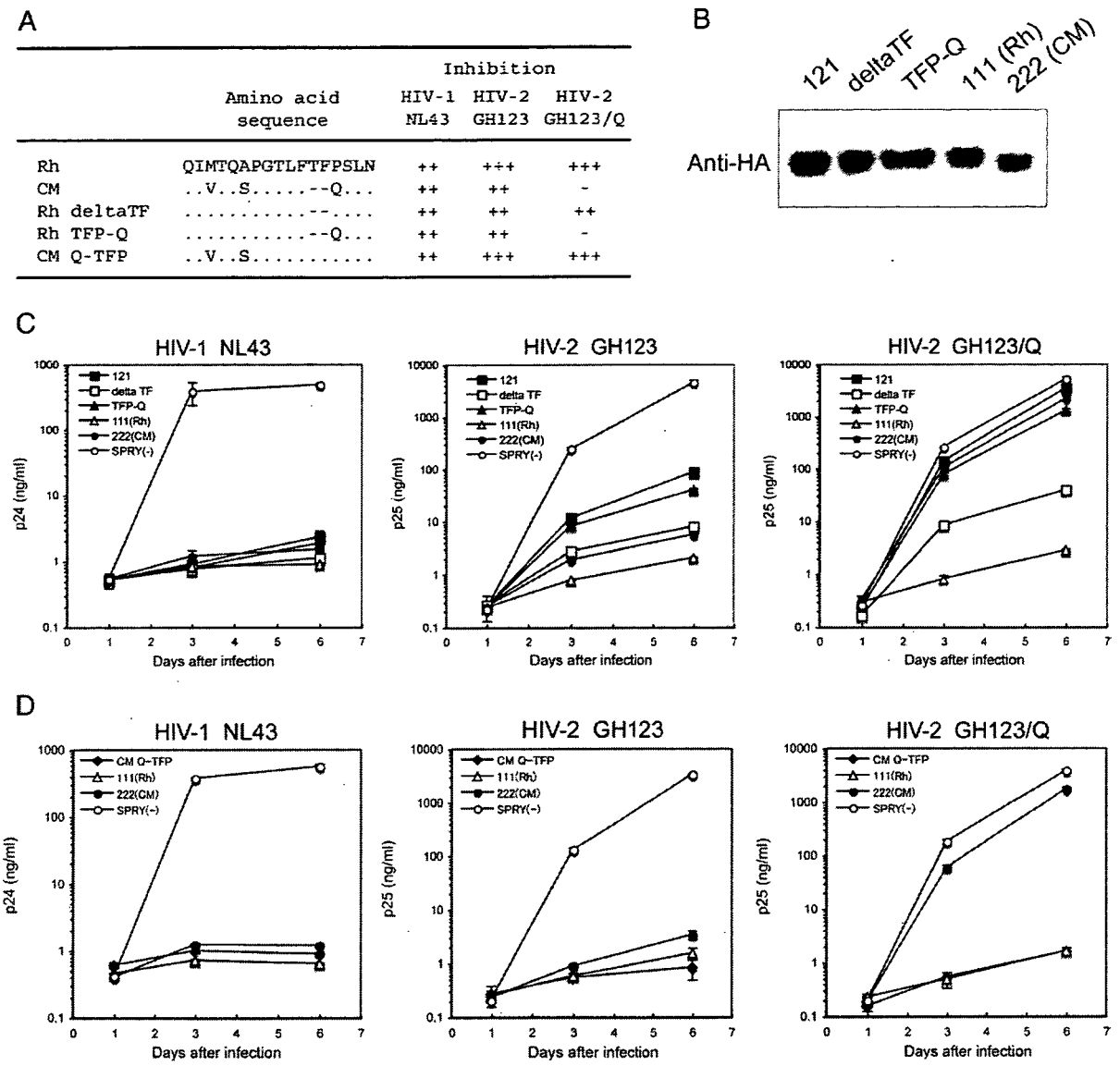

Fig. 5. (A) Mutant Rh deltaTF TRIM5α was generated by deleting 339th-TF-340th and mutant Rh TFP-Q TRIM5α was generated by replacing 339th-TFP-341st with Q by site-directed mutagenesis. Dots denote amino acid identity, dashes a lack of the amino acids residue present only in rhesus monkey (Rh) TRIM5α, and +++, ++, +, and − more than 1000-fold, 100- to 1000-fold, 8- to 100-fold, and less than 8-fold suppression of virus growth, respectively, compared with the negative control on day 6. (B) Twenty-four hours after SeV infection, TRIM5α proteins in lysates of MT4 cells infected with recombinant SeV expressing 121, Rh delta TF, Rh TFP-Q, 111 (Rh), or 222 (CM) TRIM5α were visualized by Western blotting with an antibody against HA-tag. (C) MT4 cells were infected with recombinant SeV expressing 121 (■), Rh delta TF (□), Rh TFP-Q (▲), 111 (Rh) (△), 222 (CM) (●), or CM SPRY(−) (○) TRIM5α. Nine hours after infection, cells were inoculated with HIV-1 NL43, HIV-2 GH123, or HIV-2 GH123/Q viruses. Culture supernatants were respectively assayed for levels of p24 or p25. (D) MT4 cells were infected with recombinant SeV expressing CM Q-TFP (◆), 111 (Rh) (△), 222 (CM) (●), or CM SPRY(−) (○) TRIM5α. Nine hours after infection, cells were inoculated with HIV-1 NL43, HIV-2 GH123, or HIV-2 GH123/Q viruses. Culture supernatants were respectively assayed for levels of p24 or p25.

and their reported ability to grow in these primate peripheral blood mononuclear cells.

Discussion

In the study presented here, we found that rhesus monkey TRIM5α showed anti-HIV-2 activity broader and more potent than that of cynomolgus monkey. We were also able to show that three amino acid residues TFP at the 339th to 341st positions in the V1 were important for the broad HIV-2 restriction activity of rhesus monkey TRIM5α. Previous studies have shown that the V1 of TRIM5α determines species-specific restriction of HIV-1 and SIVmac (Perez-Caballero et al., 2005; Sawyer et al., 2005; Stremlau et al., 2005; Yap et al., 2005; Nakayama et al., 2005). Ours is the first study to demonstrate that the V1 of TRIM5α also determines anti-HIV-2 potency. Since MT4 and Hut78 cells express endogenous human TRIM5α, it is possible that endogenous human TRIM5α interfere with exogenous TRIM5α. However, the expression level of SeV-derived TRIM5α is more than 100 times higher than that of endogenous TRIM5α (data

Please cite this article as: Kono, K., et al., Comparison of anti-viral activity of rhesus monkey and cynomolgus monkey TRIM5αs against human immunodeficiency virus type 2 infection, Virology (2008), doi:10.1016/j.virol.2007.12.022

not shown), and the effect of endogenous TRIM5α is therefore considered to be negligible.

A previous study using a human and rhesus monkey chimeric TRIM5α revealed that a single amino acid substitution from R to P at the 332nd position of human TRIM5α (corresponding to the 334th position in rhesus monkey TRIM5α) confers strong anti-HIV-1 activity to human TRIM5α (Stremlau et al., 2005; Yap et al., 2005). We found that rhesus monkey TRIM5α and chimeric TRIM5α containing baboon V1 strongly restricted HIV-2 GH123/Q, while chimeric TRIM5α containing sooty mangabey V1 did so only slightly, although baboon and sooty mangabey TRIM5α share the SFP motif at the 339th to 341st positions. Rhesus monkey and baboon TRIM5α possess P, whereas human and sooty mangabey TRIM5α possess R at the 334th position. On the other hand, cynomolgus monkey TRIM5α strongly restricted HIV-2 GH123, while chimeric TRIM5α containing pig-tailed monkey V1 did so only slightly. Cynomolgus monkey TRIM5α possesses P, whereas pig-tailed monkey TRIM5α possesses Q at the 334th position. These results indicate the P residue at the 334th position of primate TRIM5α also plays a critical role in the restriction of HIV-2.

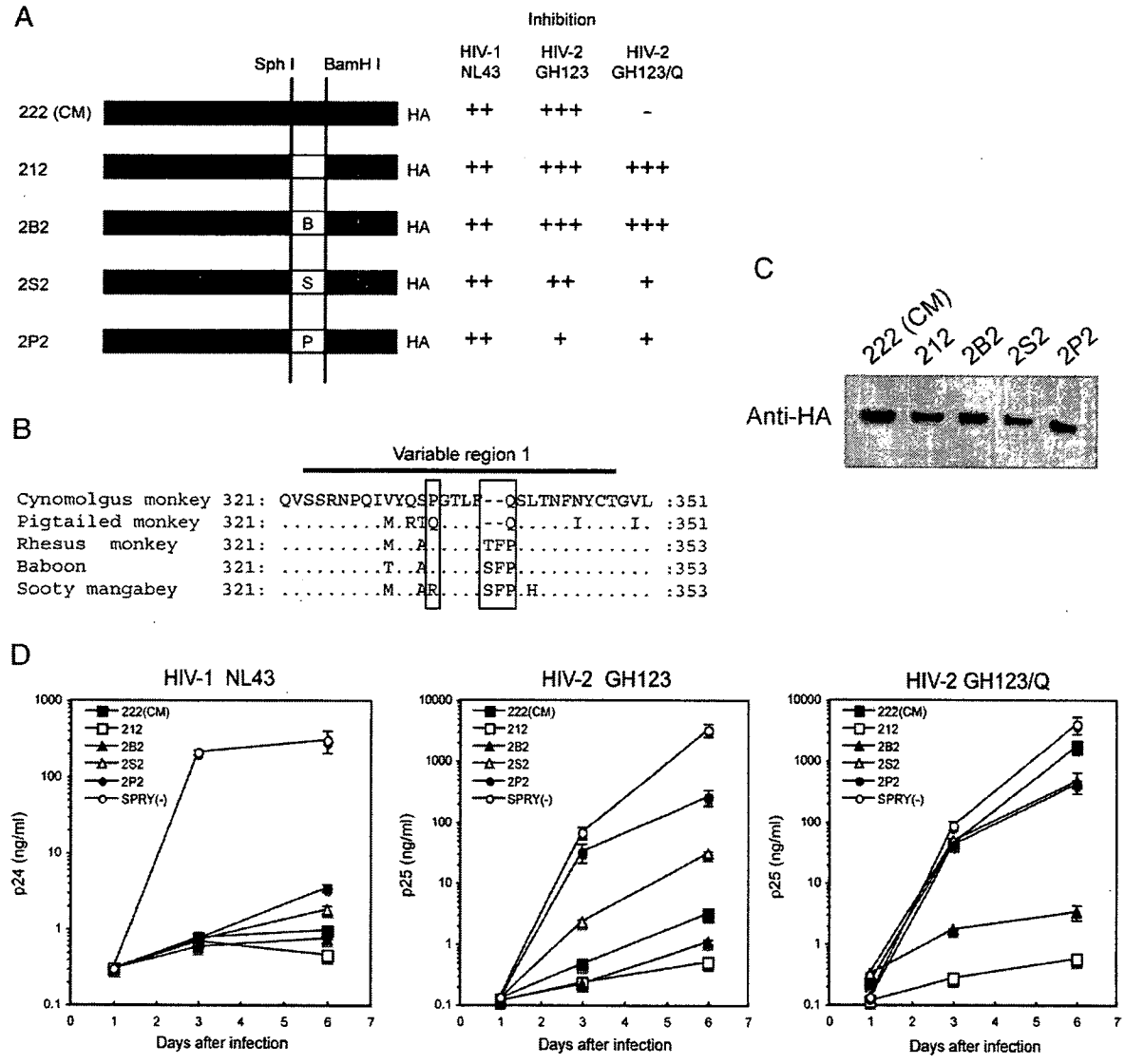

Fig. 6. (A) Schematic representation of chimeric TRIM5α and summary of the results. White and black bars denote rhesus monkey and cynomolgus monkey (CM) sequences, respectively. B, S, and P denote sequence from baboon, sooty mangabey, and pig-tailed monkey, respectively, and +++, ++, +, and − more than 1000-fold, 100- to 1000-fold, 8- to 100-fold, and less than 8-fold suppression of virus growth, respectively, compared with the negative control on day 6. (B) Alignment of amino acid sequences of the V1 and franking region within the SPRY domain of cynomolgus monkey, pigtailed monkey, rhesus monkey, baboon, and sooty mangabey TRIM5αs. V1 is indicated by a bar over the sequence. The first box indicates the amino acid residues that were referred to as site 332 in the human TRIM5α. The second box indicates amino acid residues that are important for restricting HIV-2 strains which are resistant to cynomolgus monkey TRIM5α. (C) Twenty-four hours after SeV infection, TRIM5α proteins in lysates of MT4 cells infected with recombinant SeV expressing 222 (CM), 212, 2B2, 2S2, or 2P2 TRIM5α were visualized by Western blotting with an antibody against HA-tag. (D) MT4 cells were infected with recombinant SeV expressing 222 (CM) (■), 212 (□), 2B2 (▲), 2S2 (△), 2P2 (●), or CM SPRY(−) (○) TRIM5α. Nine hours after infection, cells were inoculated with HIV-1 NL43, HIV-2 GH123, or HIV-2 GH123/Q, viruses. Culture supernatants were respectively assayed for levels of p24 or p25.

Please cite this article as: Kono, K., et al., Comparison of anti-viral activity of rhesus monkey and cynomolgus monkey TRIM5αs against human immunodeficiency virus type 2 infection, Virology (2008), doi:10.1016/j.virol.2007.12.022

HIV-2 is thought to have originated from the SIV from sooty mangabey (SIVsmm) (Hahn et al., 2000). Our results showed that HIV-2 GH123 replication was partially inhibited by chimeric TRIM5α containing sooty mangabey V1, while HIV-2 GH123/Q grew strongly in the presence of the chimeric TRIM5α. This result is consistent with the fact that all SIVsmm sequences in the Los Alamos database possess Q or A at the 119th or 120th position of CA (Song et al., 2007). On the other hand, chimeric TRIM5α containing sooty mangabey V1 has a strong anti-HIV-1 activity, even though it has R at the 334th position as in human TRIM5α. Sooty mangabey TRIM5α, on the other hand, possesses the SFP motif at the 339th to 341st positions. Yap et al. (2005) showed that human TRIM5α carrying the rhesus monkey sequence LFTFPSLT which included the TFP motif instead of the human sequence RYQTFV at the 335th to 340th positions could restrict HIV-1. These results thus indicate that the TFP or SFP motif at the 339th to 341st positions can confer anti-HIV-1 activity as well as the P residue at the 334th position.

In the case of pig-tailed monkey, which could develop an AIDS-like disease by HIV-2 (McClure et al., 2000), anti-HIV-2 activity of chimeric TRIM5α containing pig-tailed monkey V1 was very weak. Furthermore, after we completed this study, it was reported that pig-tailed monkeys lack expression of TRIM5α. Instead, pig-tailed monkeys express TRIM5θ and TRIM5η, novel TRIM5 isoforms lacking anti-HIV-1 activity (Brennan et al., 2007). These findings are probably account for the fact that pig-tailed monkey can be used as an AIDS model.

Previous studies showed that rhesus monkey as well as baboon can be infected with HIV-2 (Dormant et al., 1989; Franchini et al., 1989; Nicol et al., 1989; Franchini et al., 1990; Castro et al., 1991), while the latter can also develop an AIDS-like disease as a result of HIV-2 infection (Barnett et al., 1994; Locher et al., 1998; Locher et al., 2001). In our study, however, rhesus monkey TRIM5α and chimeric TRIM5α containing baboon V1 could strongly inhibit HIV-2 replication. The reason why HIV-2 can replicate in rhesus monkey and baboon, even though the TRIM5α of these monkey species possesses strong anti-HIV-2 activity, is unclear at present. The presence of TRIM5α mRNA in cells of rhesus monkey and baboon cells has been confirmed (Stremlau et al., 2004; Kaiser et al., 2007). It is also known that TRIM5α exhibits a high degree of sequence variation even within species. In rhesus monkey, there is a 339th-TFP-341st to Q polymorphism which diminishes the anti HIV-2 GH123/Q activity of rhesus monkey TRIM5α (Newman et al., 2006) (Fig. 5). It is thus possible that rhesus monkey carrying this polymorphism in the TRIM5α gene could be infected with HIV-2 and that a number of baboons have similar polymorphisms. It would be interesting to investigate the effect of genetic polymorphisms in baboon TRIM5α on its restriction activity against HIV-2.

Materials and methods

Cloning and expression of TRIM5α

Rhesus monkey TRIM5α cDNA was amplified by RT-PCR of mRNA extracted from rhesus monkey kidney LLC-MK2 cells using 5′-GCGGCCGCTACTATGGCTTCTGG-3′ as the forward primer and 5′-GAATTCTCAAGAGCTTGGTGA-3′ as the reverse primer. Amplified products were then cloned into the vector pCR-2.1TOPO (Invitrogen, Carlsbad, CA) and the nucleotide sequence authenticity was verified. For generating rhesus monkey TRIM5α cDNA carrying an HA tag (YPYDVPDYAA) at its C-terminus (Rh-TRIM5α-HA), cloned rhesus monkey TRIM5α cDNA in pCR-2.1TOPO was used as a template for PCR-amplification with a primer (5′-TCAAGCAGCATAATCAGGAACATCATAAGGATAAGAGCTTGGTGAGCACAGAG-3′) containing a nucleotide sequence corresponding to the HA-tag (underline) fused with the C-terminal portion of TRIM5α. The C-terminal portion of TRIM5α fused with the HA-tag (*Bam*HI to *Not*I) and the N-terminal portion of TRIM5α (*Not*I to *Bam*HI) was assembled on a pCEP4 vector (Invitrogen). Construction of cynomolgus monkey TRIM5α carrying an HA tag at the C-terminus (CM-TRIM5α-HA) was described previously (Nakayama et al., 2005).

To generate 121 chimeric TRIM5α, the 188-bp *Sph*I–*Bam*HI fragment of rhesus monkey TRIM5α was replaced with the corresponding 182-bp *Sph*I–*Bam*HI fragment of cynomolgus monkey TRIM5α in the background of Rh-TRIM5α-HA. Conversely, the 182-bp *Sph*I–*Bam*HI fragment of cynomolgus monkey TRIM5α was replaced with the 188-bp *Sph*I–*Bam*HI fragment of rhesus monkey TRIM5α in the background CM-TRIM5α-HA to generate 212 chimeric TRIM5α. To generate 112 chimeric TRIM5α, the C-terminal portion of CM-TRIM5α-HA (*Bam*HI to *Not*I) and the N-terminal portion of rhesus monkey TRIM5α were assembled on a pcDNA3.1 (−) vector (Invitrogen). Conversely, the C-terminal portion of Rh-TRIM5α-HA (*Bam*HI to *Not*I) and the N-terminal portion of cynomolgus monkey TRIM5α (*Not*I to *Bam*HI) were assembled on a pcDNA3.1 (−) vector to generate 221 chimeric TRIM5α. To generate 122 chimeric TRIM5α, the C-terminal portion of CM-TRIM5α-HA (*Sph*I to *Not*I) and the N-terminal portion of rhesus monkey TRIM5α (*Not*I to *Sph*I) were assembled on a pcDNA3.1 (−) vector. Conversely, the C-terminal portion of Rh-TRIM5α-HA (*Sph*I to *Not*I) and the N-terminal portion of cynomolgus monkey TRIM5α (*Not*I to *Sph*I) were assembled on a pcDNA vector to generate 211 chimeric TRIM5α.

Mutant rhesus monkey TRIM5α lacking two amino acid residues TF at the 339th to 340th positions (Rh deltaTF TRIM5α), mutant rhesus monkey TRIM5α in which amino acid residues TFP at the 339th to 341st positions was replaced with a single amino acid Q found in cynomolgus monkey TRIM5α (Rh TFP-Q TRIM5α), and mutant cynomolgus monkey TRIM5α in which a single amino acid Q at the 339th position was replaced with three amino acid residues TFP found in rhesus monkey TRIM5α (CM Q-TFP TRIM5α) were generated by site-directed mutagenesis by PCR-mediated overlap primer exension method (Ho et al., 1989). Briefly, two DNA fragments with overlapping ends were generated by using the outer primers and the complementary primers with overlapping complementary nucleotides containing desired mutations. The resultant two fragments were combined in the subsequent fusion reaction in which the overlapping ends anneal, allowing the 3′ overlap of each strand to serve as a primer for 3′ extension of the complementary strand. The outer primers for generating Rh deltaTF

Please cite this article as: Kono, K., et al., Comparison of anti-viral activity of rhesus monkey and cynomolgus monkey TRIM5αs against human immunodeficiency virus type 2 infection, Virology (2008), doi:10.1016/j.virol.2007.12.022

TRIM5α were 5′-GCGGCCGCTACTATGGCTTCTGG-3′ and 5′-GAATTCTCAAGAGCTTGGTGA-3′, and the complementary primers were 5′-GGGACATTATTTCCGTCACTCACG-3′ and 5′-CGTGAGTGACGGAAATAATGTCCC-3′. The outer primers were common in all cases of PCR-based mutagenesis of TRIM5α. The complementary primers for Rh TFP-Q TRIM5α were 5′-GGGACATTATTTCAATCACTCACG-3′ and 5′-CGTGAGTGATTGAAATAATGTCCC-3′ (underline; TFP-Q site), and 5′-GGACATTATTTACGTTTCCGTCACTCACG-3′ and 5′-CGTGAGTGACGGAAACGTAAATAATGTCC-3′ (underline; Q-TFP site) for CM Q-TFP TRIM5α.

2B2, 2S2, and 2P2 chimeric TRIM5α, which possessed the 188-bp *Sph*I–*Bam*HI fragment of baboon TRIM5α, 188-bp fragment of sooty mangabey TRIM5α, and 182-bp fragment of pig-tailed monkey TRIM5α, respectively, in the background of CM-TRIM5α-HA were generated by the same method as described above. To obtain *Sph*I–*Bam*HI fragments of baboon and sooty mangabey TRIM5αs, cloned rhesus monkey TRIM5α was used as a template for PCR-amplification with outer primers described above and complementary primers containing a nucleotide sequence corresponding to the 330th to 339th amino acid residues of baboon TRIM5α (5′-CAGATAACGTATCAGGCACCAGGGACATTATTTTCGTTTCCG-3′ and 5′-CGGAAACGAAAATAATGTCCCTGGTGCCTGATACGTTATCTG-3′) and the 334th to 343rd amino acid residues of sooty mangabey TRIM5α (5′-CAGGCACGAGGGACATTATTTTCGTTTCCGTCACACACGAAT-3′ and 5′-ATTCGTGTGTGACGGAAACGAAAATAATGTCCCTCGTGCCTG-3′), respectively. To obtain the *Sph*I–*Bam*HI fragment of pig-tailed TRIM5α, cloned cynomolgus monkey TRIM5α was used as a template for PCR-amplification with outer primers described above and complementary primers containing a nucleotide sequence corresponding to the 330th to 350th amino acid residues of pig-tailed monkey TRIM5α (5′-CAGTCACTCACGAATTTCATTTATTGTACTGGCATCCTGGGC-3′ and 5′-CGTGAGTGACTGAAATAATGTCCCTTGTGTCCGATACATTATCTG-3′). The entire coding sequences of those TRIM5α were then transferred to the *Not*I site of pSeV18+b(+). Recombinant SeVs carrying various TRIM5α were recovered according to a previously described method (Nakayama et al., 2005). The viruses passaged twice in embryonated chicken eggs were used as stock for all experiments.

Viral infection

2×10^5 MT4 or Hut78 cells were infected with SeV expressing each TRIM5α at a multiplicity of infection of 10 plaque-forming units per cell and incubated at 37 °C for 9 h. Cells were then superinfected with 20 ng of p24 of HIV-1 NL43, 20 ng of p27 of SIVmac239, or 20 ng of p25 of HIV-2 GH123, GH123/Q, or other HIV-2 isolates. The culture supernatants were collected periodically, and the level of p24, p27, or p25 was measured with a RETROtek antigen ELISA kit (ZeptoMetrix, Buffalo, NY).

Western blot analysis

MT4 cells infected with recombinant SeVs expressing HA-tagged TRIM5α proteins were lysed in lysis buffer (50 mM Tris–HCl, pH 7.5, 150 mM NaCl, 1% Nonident P40, 0.5% sodium deoxycholate). TRIM5α proteins in the lysates were subjected to sodium dodecyl sulfate-polyacrylamide gel electrophoresis (SDS-PAGE). Proteins in the gel were then electronically transferred to a membrane (Immobilion; Millipore, Billerica, MA). Blots were blocked and probed with anti-HA high affinity rat monoclonal antibody (Roche, Indianapolis, IN) overnight at 4 °C. Blots were then incubated with peroxidase-conjugated anti-rat IgG (American Qualex, San Clemente, CA), and bound antibodies were visualized with a Chemilumi-One chemiluminescent kit (Nacalai Tesque, Kyoto, Japan).

TRIM5α cDNA sequences

TRIM5α cDNA sequences for rhesus monkey (AY523632), cynomolgus monkey (AB210052), baboon (AY843505), sooty mangabey (AY10303), and pig-tailed monkey (AY899887–AY899893) were obtained from the GeneBank database.

Acknowledgments

The authors would like to thank Setsuko Bandou and Noriko Teramoto for their assistance. HIV-2 UC2, UC12, and UC14 viruses were kind gifts from Jay A. Levy. This work was supported by grants from the Human Health Foundation, the Ministry of Education, Culture, Sports, Science, and Technology, and the Ministry of Health, Labor and Welfare, Japan.

References

Anderson, J.L., Campbell, E.M., Wu, X., Vandegraaff, N., Engelman, A., Hope, T.J., 2006. Proteasome inhibition reveals that a functional preintegration complex intermediate can be generated during restriction by diverse TRIM5 proteins. J. Virol. 80, 9754–9760.

Barnett, S.W., Murthy, K.K., Herndier, B.G., Levy, J.A., 1994. An AIDS-like condition induced in baboons by HIV-2. Science 266, 642–646.

Berthoux, L., Sebastian, S., Sayah, D.M., Luban, J., 2005. Disruption of human TRIM5α antiviral activity by nonhuman primate orthologues. J. Virol. 79, 7883–7888.

Brennan, G., Kozyrev, Y., Kodama, T., Hu, S.L., 2007. Novel TRIM5 isoforms expressed by *Macaca nemestrina*. J. Virol. 81, 12210–12217.

Castro, B.A., Nepomuceno, M., Lerche, N.W., Eichberg, J.W., Levy, J.A., 1991. Persistent infection of baboons and rhesus monkeys with different strains of HIV-2. Virology 184, 219–226.

Diaz-Griffero, F., Li, X., Javanbakht, H., Song, B., Welikala, S., Stremlau, M., Sodroski, J., 2006. Rapid turnover and polyubiquitylation of the retroviral restriction factor TRIM5. Virology 349, 300–315.

Dormant, D., Livartowski, J., Chamaret, S., Guetard, D., Hein, D., Levagueresse, R., van de Moortelle, P.F., Larke, B., Gourmelon, P., Vazeux, R., Metivier, H., Flageat, J., Court, L., Hauw, J.J., Montagnier, L., 1989. HIV-2 in rhesus monkeys: serological, virological and clinical results. Intervirology 30, 59–65.

Franchini, G., Fargnoli, K.A., Giombini, F., Jagodzinski, L., De Rossi, A., Bosch, M., Biberfeld, G., Fenyo, E.M., Albert, J., Gallo, R.C., Wong-Staal, F., 1989. Molecular and biological characterization of a replication competent human immunodeficiency type 2 (HIV-2) proviral clone. Proc. Natl. Acad. Sci. U. S. A. 86, 2433–2437.

Franchini, G., Markham, P., Gard, E., Fargnoli, K., Keubaruwa, S., Jagodzinski, L., Robert-Guroff, M., Lusso, P., Ford, G., Wong-Staal, F., Gallo, R.C., 1990. Persistent infection of rhesus macaques with a molecular clone of human immunodeficiency virus type 2: evidence of minimal genetic drift and low pathogenetic effects. J. Virol. 64, 4462–4467.

Hahn, B.H., Shaw, G.M., De Cock, K.M., Sharp, P.M., 2000. AIDS as a zoonosis: scientific and public health implications. Science 287, 607–614.

Please cite this article as: Kono, K., et al., Comparison of anti-viral activity of rhesus monkey and cynomolgus monkey TRIM5αs against human immunodeficiency virus type 2 infection, Virology (2008), doi:10.1016/j.virol.2007.12.022

Hatziioannou, T., Perez-Caballero, D., Yang, A., Cowan, S., Bieniasz, P.D., 2004. Retrovirus resistance factors Ref1 and Lv1 are species-specific variants of TRIM5α. Proc. Natl. Acad. Sci. U. S. A. 101, 10774–10779.

Ho, S.N., Hunt, H.D., Horton, R.M., Pullen, J.K., Pease, L.R., 1989. Site-directed mutagenesis by overlap extension using the polymerase chain reaction. Gene 77, 51–59.

Kaiser, S.M., Malik, H.S., Emerman, M., 2007. Restriction of an extinct retrovirus by the human TRIM5α antiviral protein. Science 316, 1756–1758.

Keckesova, Z., Ylinen, L.M., Towers, G.J., 2004. The human and African green monkey TRIM5α genes encode Ref1 and Lv1 retroviral restriction factor activities. Proc. Natl. Acad. Sci. U. S. A. 101, 10780–10785.

Locher, C.P., Barnett, S.W., Herndier, B.G., Blackbourn, D.J., Reyes-Teran, G., Murthy, K.K., Brasky, K.M., Hubbard, G.B., Reinhart, T.A., Haase, A.T., Levy, J.A., 1998. Human immunodeficiency virus-2 infection in baboons is an animal model for human immunodeficiency virus pathogenesis in humans. Arch. Pathol. Lab. Med. 122, 523–533.

Locher, C.P., Witt, S.A., Herndier, B.G., Tenner-Racz, K., Racz, P., Levy, J.A., 2001. Baboons as an animal model for human immunodeficiency virus pathogenesis and vaccine development. Immunol. Rev. 183, 127–140.

McClure, J., Schmidt, A.M., Rey-Cuille, M.A., Bannink, J., Misher, L., Tsai, C.C., Anderson, D.M., Morton, W.R., Hu, S.L., 2000. Derivation and characterization of a highly pathogenic isolate of human immunodeficiency virus type 2 that causes rapid CD4+ cell depletion in *Macaca nemestrina*. J. Med. Primatol. 29, 114–126.

Nakayama, E.E., Miyoshi, H., Nagai, Y., Shioda, T., 2005. A specific region of 37 amino acid residues in the SPRY (B30.2) domain of African green monkey TRIM5α determines species-specific restriction of simian immunodeficiency virus SIVmac infection. J. Virol. 79, 8870–8877.

Nakayama, E.E., Maegawa, H., Shioda, T., 2006. A dominant-negative effect of cynomolgus monkey tripartite motif protein TRIM5α on anti-simian immunodeficiency virus SIVmac activity of an African green monkey orthologue. Virology 350, 158–163.

Newman, R.M., Hall, L., Connole, M., Chen, G.L., Sato, S., Yuste, E., Diehl, W., Hunter, E., Kaur, A., Miller, G.M., Johnson, W.E., 2006. Balancing selection and the evolution of functional polymorphism in Old World monkey TRIM5α. Proc. Natl. Acad. Sci. U. S. A. 103, 19134–19139.

Nicol, I., Flamminio-Zola, G., Doubouch, P., Bernard, J., Snart, R., Jouffre, R., Reveil, B., Fouchard, M., Desportes, I., Nara, P., Gallo, R.C., Zagury, D., 1989. Persistent HIV-2 infection of rhesus macaque, baboon, and mangabeys. Intervirology 30, 258–267.

Ohkura, S., Yap, M.W., Sheldon, T., Stoye, J.P., 2006. All three variable regions of the TRIM5α B30.2 domain can contribute to the specificity of retrovirus restriction. J. Virol. 80, 8554–8565.

Perez-Caballero, D., Hatziioannou, T., Yang, A., Cowan, S., Bieniasz, P.D., 2005. Human tripartite motif 5α domains responsible for retrovirus restriction activity and specificity. J. Virol. 79, 8969–8978.

Perron, M.J., Stremlau, M., Song, B., Ulm, W., Mulligan, R.C., Sodroski, J., 2004. TRIM5α mediates the postentry block to N-tropic murine leukemia viruses in human cells. Proc. Natl. Acad. Sci. U. S. A. 101, 11827–11832.

Reymond, A., Meroni, G., Fantozzi, A., Merla, G., Cairo, S., Luzi, L., Riganelli, D., Zanaria, E., Messali, S., Cainarca, S., Guffanti, A., Minucci, S., Pelicci, P.G., Ballabio, A., 2001. The tripartite motif family identifies cell compartments. EMBO J. 20, 2140–2151.

Sawyer, S.L., Wu, L.I., Emerman, M., Malik, H.S., 2005. Positive selection of primate TRIM5α identifies a critical species-specific retroviral restriction domain. Proc. Natl. Acad. Sci. U. S. A. 102, 2832–2837.

Song, B., Gold, B., O'Huigin, C., Javanbakht, H., Li, X., Stremlau, M., Winkler, C., Dean, M., Sodroski, J., 2005a. The B30.2(SPRY) domain of the retroviral restriction factor TRIM5α exhibits lineage-specific length and sequence variation in primates. J. Virol. 79, 6111–6121.

Song, B., Javanbakht, H., Perron, M., Park, D.H., Stremlau, M., Sodroski, J., 2005b. Retrovirus restriction by TRIM5α variants from Old World and New World primates. J. Virol. 79, 3930–3937.

Song, H., Nakayama, E.E., Yokoyama, M., Sato, H., Levy, J.A., Shioda, T., 2007. A single amino acid of the human immunodeficiency virus type 2 capsid affects its replication in the presence of cynomolgus monkey and human TRIM5αs. J. Virol. 81, 7280–7285.

Stremlau, M., Owens, C.M., Perron, M.J., Kiessling, M., Autissier, P., Sodroski, J., 2004. The cytoplasmic body component TRIM5α restricts HIV-1 infection in Old World monkeys. Nature 427, 848–853.

Stremlau, M., Perron, M., Welikala, S., Sodroski, J., 2005. Species-specific variation in the B30.2(SPRY) domain of TRIM5α determines the potency of human immunodeficiency virus restriction. J. Virol. 79, 3139–3145.

Stremlau, M., Perron, M., Lee, M., Li, Y., Song, B., Javanbakht, H., Diaz-Griffero, F., Anderson, D.J., Sundquist, W.I., Sodroski, J., 2006. Specific recognition and accelerated uncoating of retroviral capsids by the TRIM5α restriction factor. Proc. Natl. Acad. Sci. U. S. A. 103, 5514–5519.

Wu, X., Anderson, J.L., Campbell, E.M., Joseph, A.M., Hope, T.J., 2006. Proteasome inhibitors uncouple rhesus TRIM5α restriction of HIV-1 reverse transcription and infection. Proc. Natl. Acad. Sci. U. S. A. 103, 7465–7470.

Yap, M.W., Nisole, S., Lynch, C., Stoye, J.P., 2004. Trim5α protein restricts both HIV-1 and murine leukemia virus. Proc. Natl. Acad. Sci. U. S. A. 101, 10786–10791.

Yap, M.W., Nisole, S., Stoye, J.P., 2005. A single amino acid change in the SPRY domain of human Trim5α leads to HIV-1 restriction. Curr. Biol. 15, 73–78.

Ylinen, L.M., Keckesova, Z., Wilson, S.J., Ranasinghe, S., Towers, G.J., 2005. Differential restriction of human immunodeficiency virus type 2 and simian immunodeficiency virus SIVmac by TRIM5α alleles. J. Virol. 79, 11580–11587.

Please cite this article as: Kono, K., et al., Comparison of anti-viral activity of rhesus monkey and cynomolgus monkey TRIM5αs against human immunodeficiency virus type 2 infection, Virology (2008), doi:10.1016/j.virol.2007.12.022

JOURNAL OF VIROLOGY, Apr. 2007, p. 3757–3768 Vol. 81, No. 8
0022-538X/07/$08.00+0 doi:10.1128/JVI.01544-06

Impact of V2 Mutations on Escape from a Potent Neutralizing Anti-V3 Monoclonal Antibody during In Vitro Selection of a Primary Human Immunodeficiency Virus Type 1 Isolate[▽]

Junji Shibata,[1] Kazuhisa Yoshimura,[1] Akiko Honda,[1] Atsushi Koito,[1] Toshio Murakami,[2] and Shuzo Matsushita[1]*

Division of Clinical Retrovirology and Infectious Diseases, Center for AIDS Research, Kumamoto University, Kumamoto 860-0811,[1] and The Chemo-Sero-Therapeutic Research Institute, Kyokushi, Kikuchi, Kumamoto 869-1298,[2] Japan

Received 19 July 2006/Accepted 16 January 2007

KD-247, a humanized monoclonal antibody to an epitope of gp120-V3 tip, has potent cross-neutralizing activity against subtype B primary human immunodeficiency virus type 1 (HIV-1) isolates. To assess how KD-247 escape mutants can be generated, we induced escape variants by exposing bulked primary R5 virus, MOKW, to increasing concentrations of KD-247 in vitro. In the presence of relatively low concentrations of KD-247, viruses with two amino acid mutations (R166K/D167N) in V2 expanded, and under high KD-247 pressure, a V3 tip substitution (P313L) emerged in addition to the V2 mutations. However, a virus with a V2 175P mutation dominated during passaging in the absence of KD-247. Using domain swapping analysis, we demonstrated that the V2 mutations and the P313L mutation in V3 contribute to partial and complete resistance phenotypes against KD-247, respectively. To identify the V2 mutation responsible for the resistance to KD-247, we constructed pseudoviruses with single or double amino acid mutations in V2 and measured their sensitivity to neutralization. Interestingly, the neutralization phenotypes were switched, so that amino acid residue 175 (Pro or Leu) located in the center of V2 was exchanged, indicating that the amino acid at position 175 has a crucial role, dramatically changing the Env oligomeric state on the membrane surface and affecting the neutralization phenotype against not only anti-V3 antibody but also recombinant soluble CD4. These data suggested that HIV-1 can escape from anti-V3 antibody attack by changing the conformation of the functional envelope oligomer by acquiring mutations in the V2 region in environments with relatively low antibody concentrations.

The envelope protein (Env) of human immunodeficiency virus type 1 (HIV-1) presents on the virus surface as "spikes" composed of trimers comprising three gp120-gp41 complexes (6, 32, 33). Among the regions that induce the neutralization antibody (NAb) response, the third variable domain (V3 loop) of gp120 is considered one of the major targets of the host immune response (23, 69). It has been estimated that as much as half of the antibody response against HIV-1 Env in patient serum is directed against the V3 region (43). A recent crystallographic study revealed that the V3 loop contains features that are essential for coreceptor binding and that the extended nature and antibody accessibility of V3 are associated with its immunodominance (20).

HIV-1 primary isolates are relatively resistant to neutralization by NAbs and recombinant soluble CD4 (rsCD4) compared with variants selected for growth in permanent cell lines (42, 52, 55). Studies addressing differences between neutralization-sensitive and -resistant variants have revealed the involvement of several mechanisms that underlie the neutralization resistance of primary isolates, including the occlusion of epitopes within the oligomer, extensive glycosylation, and extension of variable loops from the surface of the complex, as well as steric and conformational blocking of receptor binding sites (7, 12, 32, 38, 49, 50, 54, 62). The structural features of gp120 tolerate a vast array of mutations that permit the selection of neutralization escape variants, as has been previously demonstrated in culture assays, animal models, and infected individuals (24).

Although there are ample data showing that NAbs can protect against HIV-1 infection in vitro and in animal models in vivo, activity in infected humans remains controversial (3, 4, 9, 14, 22, 40, 48, 58). Studies addressing NAbs in primary infections have suggested that most recently infected individuals mount a vigorous antibody response against autologous viruses. However, the rapid evolution of HIV in the presence of NAbs results in the emergence of escape mutants. As a consequence, at any time during an early stage of the HIV disease, NAbs are more likely to recognize earlier autologous viruses than contemporaneous ones. Despite evidence of phenotypic resistance, the genetic basis of the mechanism allowing primary viruses to escape from NAbs is poorly understood. Wei et al. found that glycosylation in the envelope plays an important role in allowing escape from neutralization (62). In contrast, in a recent study Frost et al. found that viral escape from NAbs is correlated with the rate of amino acid substitution rather than changes in glycosylation or insertions or deletions in the envelope (14). Because of the polyclonal nature of NAbs in patient sera, it is difficult to clarify the genetic mechanism responsible for neutralization escape.

* Corresponding author. Mailing address: Division of Clinical Retrovirology and Infectious Diseases, Center for AIDS Research, Kumamoto University, Kumamoto 860-0811, Japan. Phone: 81 96 373 6536. Fax: 81 96 373 6537. E-mail: shuzo@kaiju.medic.kumamoto-u.ac.jp.

▽ Published ahead of print on 24 January 2007.

Neutralization escape from anti-V3 monoclonal antibodies (MAbs) has been induced in T-cell-line-adapted viruses in several experiments and associated with amino acid substitution within the epitope in the V3 loop (8, 37, 65). However, Park et al. showed that human sera with neutralizing antibodies that contained polyclonal antibodies directed at the V3 region induced neutralization-resistant variants without V3 amino acid substitution (46). Neutralization studies using anti-V3 antibodies against primary isolates suggest that the neutralization resistance phenotype is associated with changes in the sequences outside V3, rather than variation within the V3 epitope (29, 62). However, the contribution of each change in the envelope to the emergence of escape mutants remains unclear because they are not selected under neutralizing MAb pressure.

Recently, we described a humanized MAb, KD-247, that displayed cross-neutralizing activity against HIV-1 clade B isolates (11). The epitope of KD-247 was mapped to six amino acids around the PGR core sequence at the tip of the V3 loop. The shortest reactive peptide recognized by KD-247 was determined to be IGPGR, which is shared by 49% of HIV-1 isolates in clade B (35). In addition, complete protection from challenge infection by a pathogenic strain of simian-human immunodeficiency virus 89.6 was observed when a high concentration of the antibody was used in an animal model (10). A molecularly cloned CCR5-tropic HIV-1 strain, JR-FL, which is relatively resistant to neutralization (15, 50), was exposed to KD-247 to obtain a neutralization escape mutant (67). Induction of the neutralization-resistant virus with a mutation in the V3 tip was observed in the presence of a high concentration of KD-247, and the escape variant was found to be more sensitive to CCR5 inhibitors and rsCD4 than the original strain (67).

The present study sought to understand how virus mutation impacts the activity of an anti-V3 MAb, KD-247. For this we subjected a primary R5 virus, MOKW, to selection pressure by KD-247. The present data suggested that it is necessary to pass a phased step so that the escape mutant against the anti-V3 antibody can emerge. Neutralization escape variants with V2 mutations in gp120 could be selected at relatively low KD-247 pressures, but high concentrations of KD-247 were required for induction of a completely resistant variant with amino acid substitution in the epitope. Moreover, we present evidence suggesting that some V2 mutations change the tertiary or quaternary structure of the envelope trimers on the viral surface that are involved in the neutralization resistance of the primary isolate. Clarification of the mechanisms responsible for this neutralization resistance may provide important insight into possible methods for the induction of potent and cross-neutralizing antibody responses capable of neutralizing various primary isolates.

(This work was presented in part at the 13th Conference on Retroviruses and Opportunistic Infection, Denver, CO, 5 to 8 February 2006 [55a].)

MATERIALS AND METHODS

Cells, culture conditions, reagents, and viruses. PM1/CCR5 cells (68) were maintained in RPMI 1640 medium (Sigma) supplemented with 10% heat-inactivated fetal calf serum (FCS; HyClone Laboratories, Logan, UT), 50 U/ml of penicillin, 50 mg/ml of streptomycin, and 100 μg/ml of G418 (Sigma). 293T cells were maintained in Dulbecco's modified Eagle medium (Sigma) supplemented with 10% heat-inactivated FCS. The CD4- and CCR5-expressing human osteogenic sarcoma cell line GHOST-hi5 was maintained in Dulbecco's modified Eagle medium supplemented with 10% FCS, G418 (200 μg/ml), hygromycin B (100 μg/ml; Sigma), and puromycin (1 μg/ml; Sigma).

KD-247, an anti-gp120-V3 antibody, was produced as previously described (11). 17b, a monoclonal antibody against the CD4-induced epitope, and immunoglobulin Gb12 (IgGb12), a monoclonal antibody against the CD4-binding epitope, were provided by the National Institutes of Health AIDS Research and Reference Reagent Program. 447-52D, an anti-gp120 V3 MAb, was a gift from Suzan Zolla-Pazner (New York University School of Medicine). 2D7, an anti-CCR5 MAb, and RPA-T4, an anti-CD4 MAb, were purchased from BD Biosciences Pharmingen (San Jose, CA). Human rsCD4 was purchased from R&D Systems, Inc. (Minneapolis, MN). TAK-779, a CCR5 inhibitor, was kindly provided by Takeda Chemical Industries, Ltd. (Osaka, Japan). AK-602, a CCR5 inhibitor, was gifted by Ono Pharmaceutical Co., Ltd. (Osaka, Japan).

The R5 primary HIV-1, MOKW virus, was isolated from a drug-naïve Japanese patient (36). This virus was passaged in phytohemagglutinin-activated peripheral blood mononuclear cells (PBMCs), and the culture supernatant was stored at −80°C until use.

Isolation of a KD-247-resistant mutant from MOKW virus in vitro. The selection of KD-247 escape variants from MOKW virus was performed as previously described (67). Briefly, MOKW virus was preincubated in the presence of KD-247 for 30 min at 37°C, and then PM1/CCR5 cells (4×10^4) were exposed to 500 times the 50% tissue culture infective dose ($TCID_{50}$) of the preincubated MOKW. After incubation for 5 h at 37°C, cells were pelleted down and resuspended in RPMI 1640 medium supplemented with 10% FCS without KD-247. Viral replication was monitored by observation of the cytopathic effects in PM1/CCR5 cells. The culture supernatant was harvested on day 7 and used to infect fresh PM1/CCR5 cells for the next round of culture in the presence of increasing concentrations of KD-247. When the virus began to propagate rapidly in the presence of KD-247, the MAb concentration was further increased. After the virus was passaged in the presence of up to 2,000 μg/ml KD-247 in PM1/CCR5 cells, a KD-247-resistant virus, MOKW9p(2000), was recovered from the cell culture supernatant. MOKW virus was also passaged for the same time period in PM1/CCR5 cells in the absence of KD-247, and the resulting virus was designated MOKW9p(−).

Amplification of viral cDNA and nucleotide sequencing. Viral RNA was extracted from cell culture supernatants with several concentrations of KD-247 using a QIAamp viral RNA kit (QIAGEN). Viral RNAs were reverse transcribed using a High Capacity cDNA Archive Kit (Applied Biosystems) with specific antisense primer ENVN (5′-CTGCCAATCAGGGAAGTAGCCTTGT GT-3′). Nested PCR was performed to amplify the gp120 C1 to C4 coding region as described previously (60). The primers used were as follows: for the first-step PCR, 1B (5′-AGAAAGAGCAGAAGACAGTGGCAATGA-3′) and H (5′-TA GTGCTTCCTGCTGCTCCCAAGAACCC-3′); for the second-step PCR, 2B (5′-AGCAGAAGACAGTGGCAATGAGAGTGA-3′) and F (5′-ATATAATT CACTTCTCCAATTGTCCCTCAT-3′). The products of the nested PCR were inserted in the TA vector (Invitrogen) and sequenced using a Big Dye Terminator, version 1.1 (Applied Biosystems), in accordance with the manufacturer's instructions.

MTT assay. The neutralization-sensitivities of each passaged MOKW virus to KD-247 were determined as previously described (67). Briefly, PM1/CCR5 cells (2×10^3 cells/well) were exposed to 100 $TCID_{50}$ of each passaged virus in the presence of various concentrations of KD-247 in 96-well round-bottom microculture plates and incubated at 37°C for 7 days. After removal of 100 μl of medium from each well, 10 μl of MTT (3-[4,5-dimethylthiazol-2-yl]-2,5-diphenyl tetrazolium bromide) solution (7.5 mg/ml) in phosphate-buffered saline (PBS) was added to each well, and the plate was incubated at 37°C for 3 h. After incubation, 100 μl of acidified isopropanol containing 4% (vol/vol) Triton X-100 was added to each well to dissolve the formazan crystals. The optical density (wavelength, 570 nm) was measured using a microplate reader. Assays were performed in duplicate or triplicate.

Construction of mutant envelope expression vectors. Proviral DNA was extracted from each batch of passaged MOKW virus-infected PM1/CCR5 cells using a QIAamp DNA blood mini kit (QIAGEN). For the construction of each passaged envelope expression vector, we used pCXN2, which has a chicken actin promoter. Briefly, we amplified MOKW gp160 regions using LA *Taq* (Takara) with primers ENVA (5′-GGCTTAGGCATCTCCTATGGCAGGAAGAA-3′) and ENVN (see above). The products of the PCR were inserted into pCR-XL-TOPO (Invitrogen). The sequences of the amplified *env* region of MOKW virus were confirmed using an ABI377 automated DNA sequencer. The EcoRI fragment of pCR-XL-MOKW containing the entire *env* region was ligated into pCXN2 to give pCXN-MOKW-RDP (the last three letters of the MOKW virus

constructs represent the amino acids at positions 166, 167, and 175 in the V2 region), pCXN-MOKW-KNL/C3m, and pCXN-MOKW-KNL/V3m. The pCXN-MOKW-KNL vector was constructed by replacing the StuI-Bsu36I fragment of pCXN-MOKW-KNL/C3m with a corresponding MOKW-RDP fragment. The pCXN-MOKW-RDP/V3m and pCXN-MOKW-RDP/C3m vectors were constructed by replacing the StuI-Bsu36I fragment of pCXN-MOKW-RDP with the corresponding pCXN-MOKW-KNL/V3m or pCXN-MOKW-KNL/C3m fragments, respectively. pCXN-MOKW-KNP, pCXN-MOKW-RDL, pCXN-MOKW-KDL, and pCXN-MOKW-RNL were generated by site-directed mutagenesis using a QuickChange Site-Directed Mutagenesis Kit (Stratagene) in accordance with the manufacturer's instructions.

Pseudovirus preparation. Five micrograms of pNL4-3.luc.R$^-$E$^-$ and 0.5 μg of pRSV-Rev (18), supplied by the NIH AIDS Research and Reference Reagent Program, and 4.5 μg of the MOKW Env-expressing pCXN2 were cotransfected into 293T cells using Effectene transfection reagent (QIAGEN). At 24 h after the transfection, the pseudovirus-containing supernatants were harvested, filtered through a 0.2-μm-pore-size filter, and stored at −80°C. To measure the pseudovirus activity, a luminescence assay using GHOST-hi5 cells was used as previously described (60).

Neutralization assays. A single-cycle infectivity assay was used to measure the neutralization of MOKW pseudoviruses as described previously (60). Briefly, MAbs at various concentrations and a pseudovirus suspension corresponding to 100 $TCID_{50}$ were preincubated on ice for 15 min. The virus-antibody mixtures were added to GHOST-hi5 cells, which on the preceding day had been seeded in a 96-well plate (1.5×10^4 cells/well). Cultures were incubated for 2 days at 37°C, washed with PBS, and lysed with lysis buffer (Luc PGC-50; PicaGene). Following transfer of the cell lysates to luminometer plates (Coastar 3912), the luciferase activity (in relative light units) in each well was measured using luciferase substrate (100 μl/well; PicaGene) in a TR717 microplate luminometer (Applied Biosystems). The reduction in infectivity was determined by comparing the relative light units in the presence and absence of MAbs and was expressed as the percentage of neutralization. The same assay was repeated two to three times.

In vitro binding assay to the MOKW envelope-expressing cell surfaces. In vitro binding assays were performed as previously described (53, 67). EcoRI fragments of MOKW *env* genes from pXL-MOKWs were subcloned into the corresponding sites in pDNR-1r (Clontech). The vectors were sequenced to confirm the presence of the desired *env* gene and the absence of other changes. The *env* gene fragments were then subcloned into pLP-IRES2-EGFP (Clontech) using Cre-recombinase (Clontech) in accordance with the manufacturer's instructions. 293T cells were cotransfected with pRSV-Rev (0.5 μg) and pLP-IRES2-EGFP-MOKW (9.5 μg) using the Effectene transfection reagent. After 36 h, the cells were harvested, incubated with each anti-HIV-1 MAb in combination with biotin-conjugated anti-human IgG and peridinin chlorophyll protein-conjugated streptavidin (BD Pharmingen), gated for the green fluorescent protein (GFP)-positive area, and analyzed using a FACSCalibur flow cytometry system.

MAb-gp120 binding assay. Culture supernatants containing the pseudotyped viruses were treated with 1% nonionic Nonidet P-40 to provide a source of gp120. Binding assays for MAbs to gp120 were then performed essentially as described elsewhere (41, 59). Briefly, gp120 proteins from transfected culture supernatants, diluted in Tris-buffered saline containing 10% FCS and 1% Nonidet P-40, were captured onto solid phase via their carboxyl termini using sheep polyclonal antibody D7324 (Aalto Bioreagents, Dublin, Ireland). MAb was added in PBS containing 10% FCS and 0.1% nonionic detergent Tween 20, and bound MAb was detected with alkaline phosphatase-conjugated goat anti-human IgG (Sigma) followed by the addition of phosphatase substrate (Sigma). A_{405} measurements were taken using a microplate reader.

Construction of chimeric NL4-3/MOKW *env* proviruses. Chimeric proviruses were constructed from the pNL4-3 proviral plasmid (AIDS Research and Reference Reagent Program, National Institute of Allergy and Infectious Diseases) by overlapping PCR as previously described, with minor modifications (31). Briefly, the gp160 coding sequences were amplified from the cloning vectors using the primers EnvFv (5′-AGCAGAAGACAGTGGCAATGAGAGCGAAG-3′) and EnvR (5′-TTTTGACCACTTGCCACCCATCTTATAGC-3′). A portion of the NL4-3 provirus from nucleotides 5284 to 6232 was amplified with primers NL(5284)F (5′-GGTCAGGGAGTCTCCATAGAATGGAGG-3′) and NL(6232)Rv (5′-CTTCGCTCTCATTGCCACTGTCTTCTGCT-3′). This fragment encompasses the unique EcoRI restriction site in pNL4-3. Another fragment from the NL4-3 provirus spanning nucleotides 8779 to 9045 was amplified using the primers NL(8779)F (5′-GCTATAAGATGGGTGGCAAGTGGTCAAAA-3′) and NL(9045)R (5′-GATCTACAGCTGCCTTGTAAGTCATTGGTC-3′). This fragment includes the unique XhoI restriction site in pNL4-3. Overlapping PCR was used to join the gp160 coding sequence from the desired clone to the fragment encompassing bases 8779 to 9045 that had been amplified from pNL4-3. The resulting fragment was then similarly joined to the amplified fragment encompassing bases 5284 to 6232 from pNL4-3. The product was digested with EcoRI and XhoI and subcloned into the corresponding site in pBluescript SK(+) (Stratagene) for sequencing and subsequent manipulation. The EcoRI-XhoI fragment for each *env* gene was then subcloned back into pNL4-3. The results were proviral plasmids that differed from each other only in the *env* gene. The resulting plasmids were designated pNL-MOKW-RDL and pNL-MOKW-KNL.

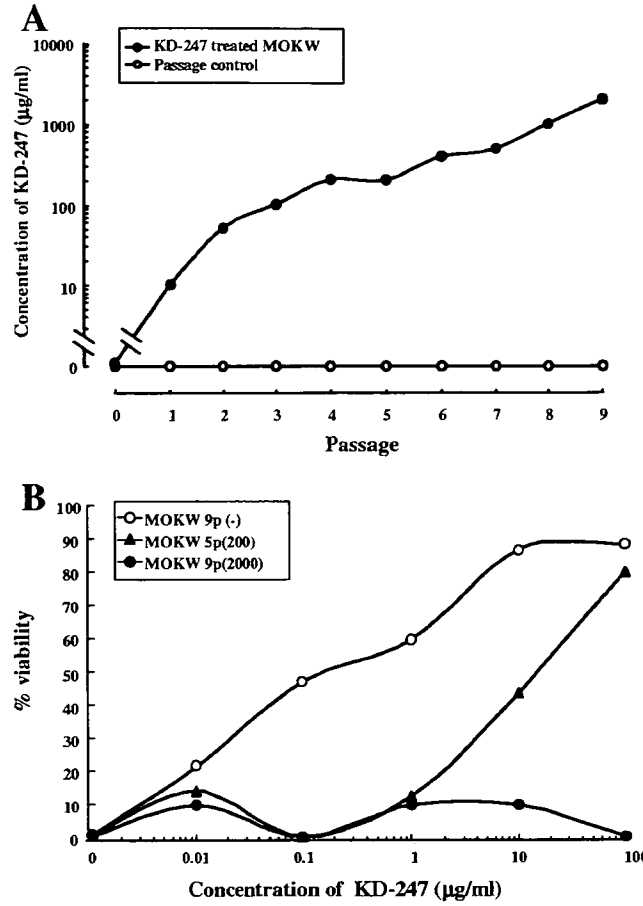

FIG. 1. Selection of neutralization-resistant virus variants against KD-247. (A) The selection was carried out in PM1/CCR5 cells, as described in Materials and Methods. (B) Sensitivity of MOKW5p(200) and MOKW9p(2000) virus to KD-247 as determined by MTT assay. PM1/CCR5 cells (2×10^3) were exposed to 100 $TCID_{50}$ of MOKW9p(−), MOKW5p(200), or MOKW9p(2000) virus and were cultured in the presence of various concentrations of KD-247. The IC_{50} values were determined by MTT assay on day 7 of culture. The assay was conducted in duplicate. The values shown are representative of three separate experiments.

Virus preparation and viral replication assay in PM1/CCR5 cells. Three micrograms of pNL-MOKW-RDL or pNL-MOKW-KNL was transfected into 293T cells using the Effectene transfection reagent. At 24 h after transfection, the virus-containing supernatants were harvested, filtered through a 0.2-μm-pore-size filter, and frozen in aliquots at −150°C. Viral yields were quantified by a RETROtek HIV-1 p24 antigen enzyme-linked immunosorbent assay (ELISA) kit (ZeptoMetrix). PM1/CCR5 cells (1×10^4) were exposed to NL4-3/MOKW *env* chimeric viruses corresponding to 10 ng of p24 and then preincubated for 4 h at 37°C. After incubation, cells were pelleted down and resuspended in RPMI 1640 medium supplemented with 10% FCS. Viral replication was monitored by measuring p24 kinetics in duplicate.

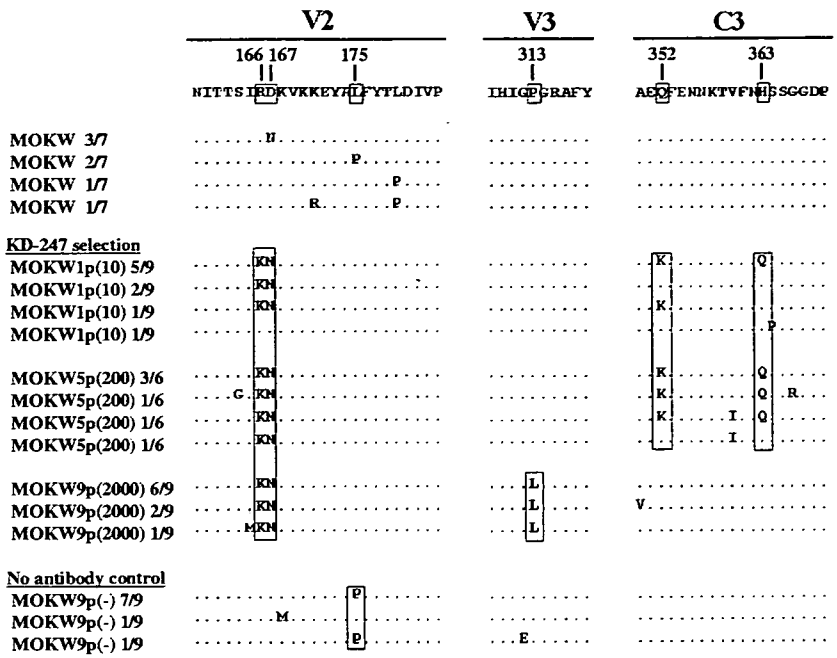

FIG. 2. Amino acid sequences of gp120 from the supernatants of MOKW-infected PM1/CCR5 cells passaged in the presence or absence of KD-247. Viral RNA from the cell culture supernatants at several concentrations of KD-247 was reverse transcribed. After the obtained cDNAs were subjected to PCR amplification and cloning, the *env* regions in the viruses passaged in the presence or absence of KD-247 were sequenced. The V2, V3, and C3 regions are indicated. The top amino acid sequence represents one of the major sequences from supernatants of MOKW-infected PBMCs. The locations and numbers of specific amino acids, based on the HXB2 sequence, are shown above the consensus line. The number of clones with the listed sequence among the total number of clones tested is given after each designation. For each set of clones, the deduced amino acid sequence of the gp120 was aligned by the single amino acid code. Dots denote sequence identity.

Nucleotide sequence accession numbers. Nucleotide sequences have been deposited in the DNA Data Bank of Japan under accession numbers AB262847 to AB262951 (passaged samples) and AB262952 to AB262961 (*env* expression vectors).

RESULTS

Anti-HIV-1 activity of KD-247 for the primary R5 isolate, MOKW virus. KD-247 recognized an epitope that contains the IGPGR sequence located at the tip of V3 and neutralized primary HIV-1 in clade B with matching sequence motifs (11). To study how bulked primary R5 virus can escape from anti-V3 antibody, we selected a genetically heterogenous HIV-1 primary isolate, MOKW, rather than a molecular clone to allow escape mutants to be selected from a quasi-species pool as well as to be generated de novo. MOKW virus was isolated by standard PBMC culture from a drug-naïve Japanese patient infected with HIV-1 by heterosexual contact (36). The isolate was sensitive to neutralization by KD-247 with a 50% inhibitory concentration (IC_{50}) of 3.4 μg/ml, which is comparable to the IC_{50} values of the Ba-L, JR-FL, and 89.6 viruses (data not shown).

Selection of KD-247 escape mutants from MOKW virus. To select an HIV-1 variant that could escape neutralization by KD-247 in vitro, we exposed PM1/CCR5 cells to MOKW virus and serially passaged the virus in the presence of increasing concentrations of KD-247. PM1/CCR5 cells were highly sensitive to both X4 and R5 HIV infection and were accompanied by prominent syncytia (68). As a control, MOKW virus was passaged under the same conditions but without KD-247 to allow us to monitor spontaneous changes that occurred in the virus during prolonged PM1/CCR5 cell passaging. The selected virus was initially propagated in the presence of 10 μg/ml KD-247, and during the course of the selection procedure, the MAb concentration was increased to 2,000 μg/ml (Fig. 1A). After five rounds of passaging, a viral variant, designated MOKW5p(200), arose that replicated in the presence of 200 μg of KD-247 per ml. Moreover, after nine rounds of passaging, a viral variant, designated MOKW9p(2000), arose that infected PM1/CCR5 cells efficiently in the presence of 2,000 μg/ml KD-247 (Fig. 1A). We harvested each passaged virus and a passaged control virus, designated MOKW9p(−), and evaluated their sensitivity to KD-247 using the MTT assay (Fig. 1B). The IC_{50} values of KD-247 against the MOKW9p(−), MOKW5p(200), and MOKW9p(2000) viruses were 0.15 μg/ml, 16 μg/ml, and >100 μg/ml, respectively, indicating that MOKW virus had acquired a resistance phenotype against KD-247 during the in vitro selection.

Sequences of the envelope region of the KD-247 escape mutants. To determine the genetic basis underlying the resistance of the variant MOKW strains, the *env* gene was amplified and sequenced. The C1 to C4 regions of the envelope were sequenced after cloning the PCR product for each region using cDNAs synthesized from viral RNAs obtained from the supernatants of infected cells, as previously described (67). A total of six to nine clones for each sample from PCR products from the passaged viruses were isolated and sequenced.

Before selection by KD-247 was begun, the V2 regions of MOKW *env* had variable amino acid sequences (Fig. 2). In

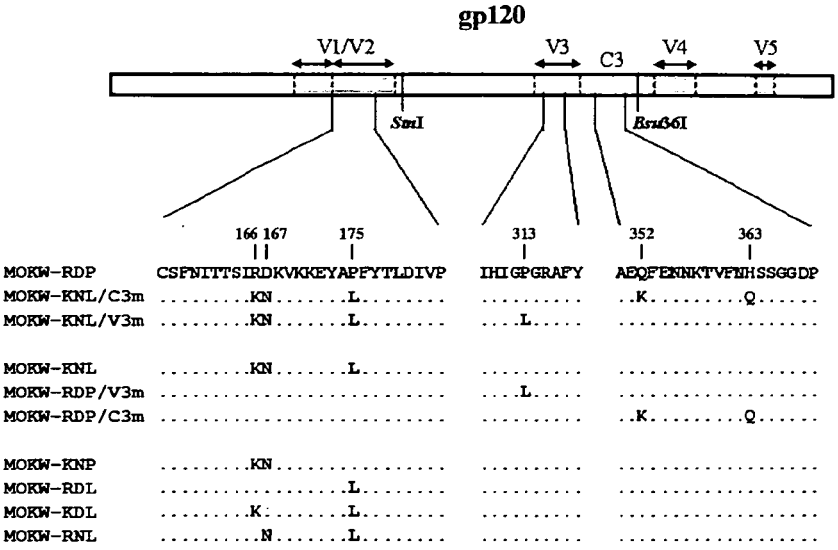

FIG. 3. Schematic representation of recombinant MOKW *env* genes used for analysis of the genetic basis for resistance to KD-247. MOKW-RDP, MOKW-KNL/C3m, and MOKW-KNL/V3m *env* genes were amplified from passaged MOKW virus-infected PM1/CCR5 cells in the absence or presence of KD-247. MOKW-KNL, MOKW-RDP/V3m, and MOKW-RDP/C3m *env* genes were constructed by replacing each region of MOKW-RDP with the corresponding MOKW-KNL/C3m or MOKW-KNL/V3m sequence. MOKW-KNP, MOKW-RDL, MOKW-KDL, and MOKW-RNL viruses were constructed by site-directed mutagenesis. Construction of the clones and mutagenesis procedures are described in Materials and Methods. The locations and numbers of specific amino acids, based on the HXB2 sequence, are shown above the MOKW-RDP sequence.

the first passage, two amino acid mutations in the V2 region and two amino acid mutations in the C3 region (five of nine clones) appeared, and after the fifth passage, the ratios of V2 and C3 mutated variants had further increased (seven of eight clones). However, after the ninth passage, the C3 mutations had completely disappeared, and a Pro-to-Leu substitution (P313L) in the V3 tip emerged in addition to the mutations in the V2 region (Fig. 2). The appearance of escape mutants with a V3 tip mutation was anticipated, because prior studies on the profile of KD-247 binding to peptides suggested that amino acid substitution at the V3 tip abrogates MAb binding (11). Some changes in the envelope sequence in other regions, including C1, V1, C2, V4, and C4, of the escape mutant were found even at early time points in the presence of the selective pressure. It is possible that these mutations also confer resistance to KD-247 but lead to viruses with decreased fitness, and thus they did not expand in the subsequent passage (Fig. 2 and data not shown). The virus passaged in PM1/CCR5 cells without KD-247 did not show the P313L substitution at passage 9 (zero of nine clones) (Fig. 2). However, accumulation of a mutation of leucine to proline at position 175 (L175P) in the V2 region was observed in the culture without KD-247. This mutation was not found in any passaged variants with KD-247.

Neutralization sensitivities of mutated MOKW pseudoviruses. To determine which substitutions were responsible for KD-247 resistance, we constructed luciferase-reporter viruses which were pseudotyped with the representative envelopes of MOKW5p(200), MOKW9p(2000), and passaged viruses without KD-247 [MOKW9p(−)], and were designated MOKW-KNL/C3m, MOKW-KNL/V3m, and MOKW-RDP virus, respectively (Fig. 3). Chimeric envelopes were constructed by replacing the mutated-region (V2, V3, or C3) with a corresponding MOKW-RDP virus (designated MOKW-KNL, MOKW-RDP/V3m, and MOKW-RDP/C3m, respectively), and then sensitivity was compared with that of the passaged virus without KD-247. As shown in Fig. 4, the V3-tip-mutated pseudoviruses, MOKW-KNL/V3m and MOKW-RDP/V3m, were completely resistant to KD-247 (>25,000-fold), whereas V2-mutated viruses, MOKW-KNL/C3m and MOKW-KNL, were only partially resistant (125-fold and 500-fold, respectively) (Fig. 4 and Table 1). The involvement in neutralization resistance of mutation in the V1/V2 region has been reported by number of researchers (12, 49, 50, 54). Our results show that the MOKW variants that had V2 mutations and a resistance phenotype against KD-247 were selected under pressure from relatively low concentrations of KD-247 (10 to 200 μg/ml) and that evolution of fully resistant variants with a mutation in the V3 tip was observed under pressure from high concentrations of the antibody.

We then determined whether the KD-247 escape variants remained sensitive to other neutralizing antibodies (447-52D and 17b), rsCD4, anti-CCR5 antibody (2D7), anti-CD4 antibody (RPA-T4), and the small-molecule CCR5 inhibitor (TAK-779) (Fig. 4 and Table 1). The KD-247 escape variants with the P313L mutation, MOKW-KNL/V3m and MOKW-RDP/V3m, were also resistant to another anti-V3 MAb, 447-52D, and V2-mutated viruses without V3 mutation, MOKW-KNL/C3m and MOKW-KNL, were partially resistant (the same as for KD-247). In contrast, the V2-mutated viruses (MOKW-KNL/C3m, MOKW-KNL/V3m, and MOKW-KNL) showed resistance to rsCD4 and 17b (a MAb to the CD4-induced epitope; CD4i) compared with the pseudoviruses without V2 mutations, i.e., MOKW-RDP, MOKW-RDP/C3m, and MOKW-RDP/V3m. Moreover, the pseudoviruses with V3 tip mutations, MOKW-KNL/V3m and MOKW-RDP/V3m, be-

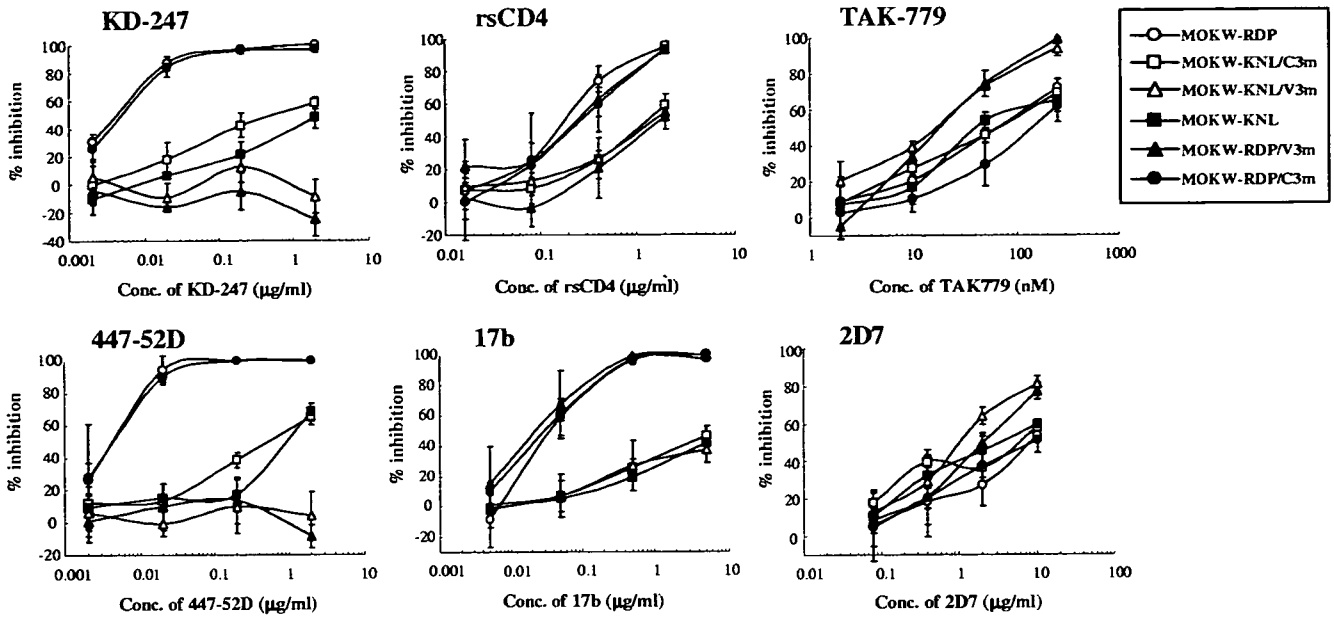

FIG. 4. Neutralization sensitivities of pseudoviruses with *env* genes from passaged MOKW viruses to MAbs, rsCD4, and CCR5 inhibitors. Pseudoviruses with the envelope sequences listed on the figure were prepared as described in Materials and Methods. KD-247, 447-52D, rsCD4, and 17b were preincubated with 100 $TCID_{50}$ of each MOKW pseudotype virus for 15 min, followed by the addition of the mixtures to the target cells (GHOST-hi5). The target cells were treated with TAK-779 and 2D7 for 15 min, followed by inoculation of the pseudotype clones. The inhibitory effects were determined by measuring the luciferase activities on day 2 of culture. Conc, concentration.

came significantly more sensitive to TAK-779 and 2D7 compared with pseudoviruses without the P313L mutation (Fig. 4 and Table 1). No significant differences with respect to sensitivity to RPA-T4 were observed between any pseudoviruses (Table 1). These data indicate that V3 tip and V2 mutations confer neutralization resistance against anti-V3 antibodies and that these mutations affect viral sensitivity to neutralizing antibodies recognizing different epitopes and anti-CCR5 antibody/agents.

Binding affinity of neutralizing antibodies to MOKW Env proteins on the cell surface. To elucidate the mechanism by which escape virus variants with V3 tip and V2 mutations become less sensitive to neutralizing antibodies, MOKW Env-expressing 293T cells were established by transfection with each Env expression plasmid and then stained with the MAbs. Binding of KD-247, 447-52D, and 17b to the surface-expressed Env proteins was assayed using fluorescence-activated cell sorter (FACS) analysis. As shown in Fig. 5A, the mean fluorescence intensities (MFIs) of KD-247 binding to the Env proteins without either V2 or V3 mutations (the MOKW-RDP and MOKW-RDP/C3m cells) were 30.13 and 29.20, respectively. However, the corresponding values for the V3-tip-mutated Env-expressing cells (MOKW-KNL/V3m and MOKW-RDP/V3m) were almost the same as negative controls (6.90 and 6.66, respectively). The MFI of the V2-mutated Env-expressing cells (MOKW-KNL/C3m and MOKW-KNL) indicated a lower binding affinity (17.89 and 19.18, respectively) than for Env proteins without V2 and V3 mutations. The binding pattern of 447-52D to these Env-expressing cells was similar to that of KD-247 (Fig. 5B). However, reduction in the binding of 17b was observed for strains with V2-mutated Env proteins (MOKW-KNL/C3m, MOKW-KNL/V3m, and

TABLE 1. Anti-HIV-1 activities of various MAbs and inhibitors toward MOKW pseudoviruses

Class	Compound	IC_{50} (μg/ml) of the indicated virus (relative IC_{50})[a]					
		MOKW-RDP	MOKW-KNL/C3m	MOKW-KNL/V3m	MOKW-RDP/C3m	MOKW-KNL	MOKW-RDP/V3m
V3 MAbs	KD-247	0.004 (1)	0.5 (125)	>100 (>25,000)	0.005 (1.3)	2 (500)	>100 (>25,000)
	447-52D	0.004 (1)	0.5 (125)	>2 (>500)	0.004 (1)	0.8 (200)	>2 (>500)
CD4-induced MAb	17b	0.035 (1)	>5 (>143)	>5 (>143)	0.03 (0.86)	>5 (>143)	0.02 (0.57)
CD4	rsCD4	0.18 (1)	1.3 (7.22)	1.5 (8.33)	0.24 (1.33)	1.8 (10)	0.24 (1.33)
CCR5 MAb	2D7	8 (1)	6.8 (0.85)	1 (0.13)	8 (1)	3.2 (0.4)	2 (0.25)
CCR5 inhibitor	TAK-779	63 (1)	63 (1)	18 (0.29)	140 (2.22)	65 (1)	18 (0.29)
CD4 MAb	RPA-T4	0.4 (1)	0.26 (0.65)	0.22 (0.55)	0.5 (1.25)	0.22 (0.55)	0.44 (1.1)

[a] GHOST-hi5 cells were exposed to 100 $TCID_{50}$ of each MOKW pseudovirus and then cultured in the presence of various concentrations of MAb or inhibitors. The IC_{50} values were determined using the luciferase reporter assay on day 2 of culture. All assays were conducted in triplicate. The value in parentheses is the ratio of the IC_{50} of the compound to the IC_{50} of the MOKW-RDP virus. Values for the compound TAK-779 are nanomolar concentrations. Data shown are representative of two or three separate experiments.

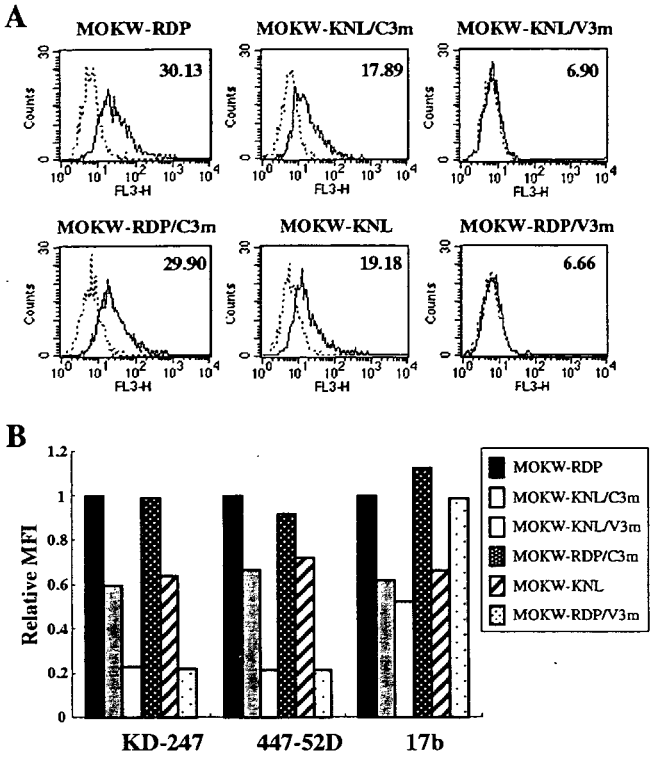

FIG. 5. Comparison of antibody binding to cell surface-expressed MOKW Env proteins. (A) 293T cells transfected with MOKW Env expression vectors were harvested at 24 h posttransfection and stained with KD-247. Flow cytometry data for binding of the KD-247 (black lines) to cell surface MOKW Env proteins are shown among GFP-gated 293T cells along with the control antibody (normal human IgG; dotted lines). The number at the top right of each graph is the MFI. (B) Each bar indicates the relative binding of KD-247, 447-52D, and 17b to MOKW Env-expressing cell surfaces. Data were normalized to each antibody's MFI for MOKW-RDP virus. FL3-H, relative fluorescence.

MOKW-KNL), whereas no difference in 17b binding was noted for the V3-mutants without V2 mutations (Fig. 5B). These findings are consistent with the results of a single-round neutralization assay (Fig. 4). Taken together, these data suggest that the mutations in V2 have a significant influence on access by antibodies to V3 as well as to the CD4i epitope. This is because access by antibodies to the epitopes of the functional envelope is related to neutralization sensitivity or resistance.

Identification of the V2 region site responsible for the neutralization resistance phenotype by site-directed mutagenesis of specific residues. Because KD-247 recognizes an epitope containing the IGPGR amino acid sequence in the V3 tip, the MAb could not bind the V3 tip of mutated Env proteins. Consequently, KD-247 does not neutralize V3-tip-mutated virus strains (67). However, the mechanism of neutralization resistance associated with V2 mutations is not known. To clarify the responsible mutation in the V2 region that confers the escape phenotype with respect to KD-247, we introduced V2 amino acid changes individually and in combination into the MOKW-RDP Env expression vector (Fig. 3) and measured the sensitivities of pseudoviruses with these envelopes to KD-247. As shown in Fig. 6, the R166K/D167N double mutant, MOKW-KNP virus, showed almost the same neutralization sensitivity as MOKW-RDP virus against KD-247. Surprisingly, a single amino acid change (P175L in MOKW-RDL) was sufficient to confer >10,000-fold resistance upon MOKW-RDP virus, with an IC_{50} of >100 μg/ml. R166K/P175L (MOKW-KDL) mutations also conferred resistance. Both the MOKW-RDL and MOKW-KDL viruses were much more resistant than the fully V2-mutated virus, MOKW-KNL (>100-fold and >10-fold resistance, respectively) (Fig. 6). The D167N/P175L (MOKW-RNL) mutant was more resistant than MOKW-KNL virus (10-fold) but less resistant than the MOKW-RDL and MOKW-KDL viruses. We also constructed a V2 mutant of JR-FL and confirmed that JR-FL with an amino acid substitution of Leu to Pro at position 175 became highly sensitive to KD-247 compared with JR-FL with Leu at position 175 in Env (data not shown). These results suggest that residue 175 (Pro or Leu) is the crucial amino acid for determining neutralization sensitivity against KD-247 and that the phenotypic influence of the R166K and D167N changes is strictly context dependent, requiring the presence of Leu at residue 175.

We then determined whether these pseudoviruses with various V2 mutations remained sensitive to other neutralizing antibodies (447-52D and IgGb12), rsCD4, 2D7, RPA-T4, and TAK-779 (Fig. 6). MOKW-RDL and MOKW-KDL viruses were also resistant to another anti-V3 MAb, 447-52D, CD4 binding site MAb, IgGb12, and rsCD4. MOKW-RNL was partially resistant compared with MOKW-KNL but less resistant than MOKW-RDL and MOKW-KDL against 447-52D, IgGb12, and rsCD4. These results were similar to those for KD-247. All V2-mutated clones were sensitive to TAK-779 and 2D7, as was MOKW-RDP virus (Fig. 6 and data not shown). However, the anti-CD4 MAb RPA-T4 neutralized both the MOKW-RDL and MOKW-KDL viruses at an approximately threefold lower concentration than other viruses (Fig. 6). These results suggest that the amino acids at positions 166 and 167 (with RD and KN sequences) may help compensate for any reduced fitness of viruses with Leu at residue 175. On the other hand, Pro at position 175 in MOKW-RDP virus might be accumulated because it confers better fitness to replicate on PM1/CCR5 cells in the absence of KD-247 pressure.

Binding affinity of MAbs against monomeric or cell surface-expressed gp120 with mutations in V2. To determine the difference in binding of MAbs to monomeric gp120 of MOKW Env with V2 mutations relative to that of MOKW-RDP virus, we performed MAb binding assays. Monomeric gp120 was prepared from pseudoviruses that had a series of V2 mutations and was captured on an ELISA plate, followed by detection by MAbs. No difference was noted in the binding activity of KD-247 or 447-52D to monomeric gp120 from V2-mutated and MOKW-RDP envelopes (Fig. 7). These results suggest that V2-mutated Env proteins retain the neutralizing epitope at least in monomeric gp120.

In contrast to the monomeric form, gp120 expressed on the cell surface contained, to a certain degree, functional envelope oligomers that were directly related to the infectivity and neutralization sensitivity of the virus. To compare the binding activity of MAbs for the surface-expressed Env with the results obtained for monomeric gp120, 293T cells transfected with MOKW-RDP and MOKW-KNP viruses, a V2 mutant strain, were subjected to FACS analysis. As shown in Fig. 8A and B,

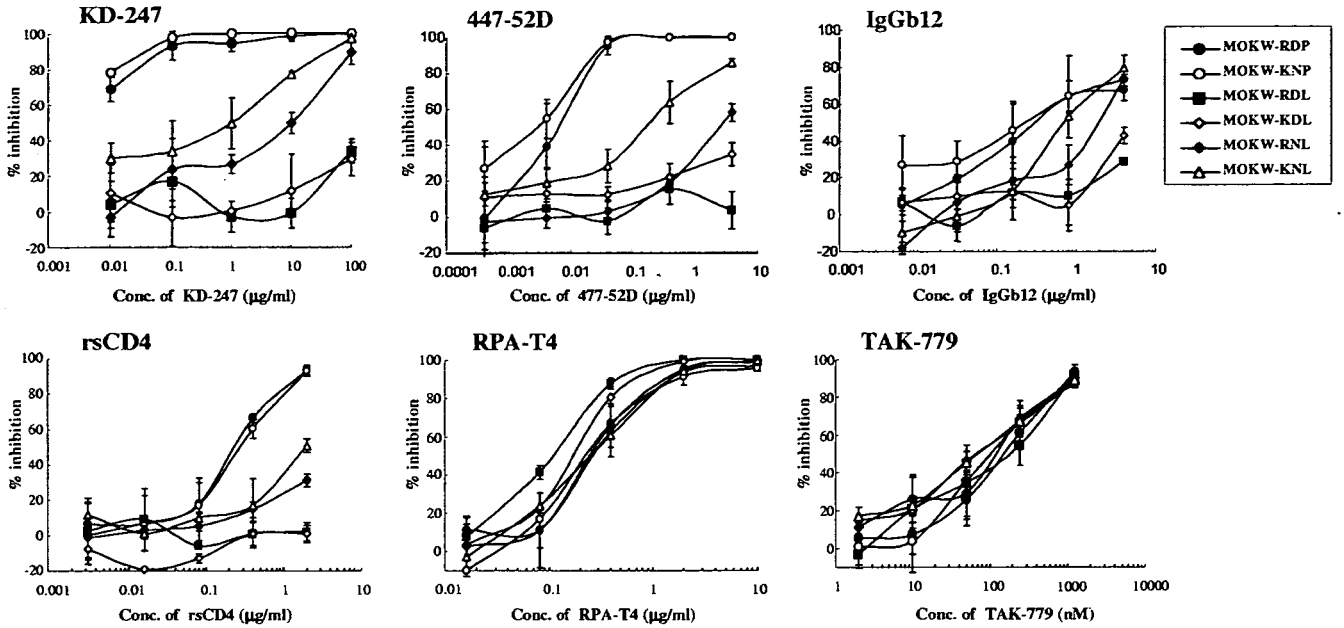

FIG. 6. Neutralization sensitivities of pseudoviruses with *env* genes from MOKW9C(−) virus with selected V2 mutations to MAbs, rsCD4, and CCR5 inhibitors. Pseudoviruses that have envelope sequences with the selected V2 mutations listed on Fig. 4 were prepared as described in Materials and Methods. KD-247, 447-52D, rsCD4, and IgGb12 were preincubated with 100 $TCID_{50}$ of each MOKW pseudotype virus for 15 min, followed by addition of the mixtures to the target cells (GHOST-hi5). Target cells were treated with TAK-779 and RPA-T4 for 15 min, followed by inoculation of the pseudotype clones. Inhibitory effects were determined by measuring the luciferase activities on day 2 of culture. Conc, concentration.

the relative binding of KD-247, 447-52D, and IgGb12 to Env expressed on the cell surface was no different than for MOKW-RDP and MOKW-KNP.

Consistent with the results of the single-round neutralization assay shown in Fig. 6, MOKW-RDL virus had the lowest binding affinity for all tested MAbs. To determine which mutations (166K or 167N) further influence binding affinity, in addition to the MOKW-RDL background, we constructed MOKW-KDL and MOKW-RNL Env proteins and measured the binding affinity by FACS. The MOKW-KDL Env was found to have a slightly greater binding affinity for KD-247, 447-52D, and IgGb12 than MOKW-RDL Env. But cell surface binding of all tested MAbs to MOKW-RNL was better than for MOKW-KDL. The strain with a fully V2-mutated Env, MOKW-KNL, had a binding profile that was intermediate between single- or double-mutated Env proteins and nonmutated Env, but in the case of IgGb12, the binding affinity of MAbs for MOKW-KNL was comparable to that for MOKW-RDP. These data were consistent with the results obtained from the neutralizing assay using a high concentration of each MAb (Fig. 6).

Comparison of replication kinetics between the NL-MOKW-RDL and NL-MOKW-KNL viruses. Although the MOKW-RDL variant was much more resistant against KD-247 than the MOKW-KNL variant (Fig. 6) and the RD sequence was

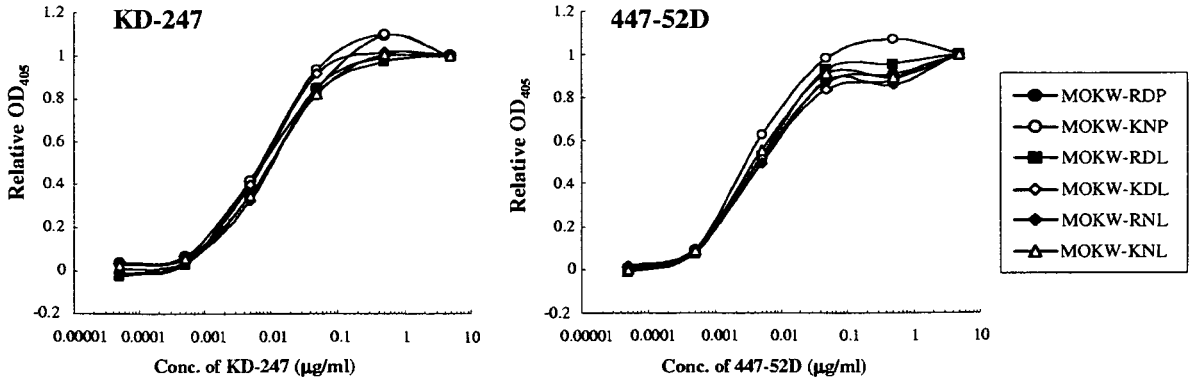

FIG. 7. Binding affinity of anti-V3 MAbs to monomeric gp120. Viral lysates for each MOKW pseudovirus were used. gp120 was captured onto microtiter wells using a sheep polyclonal antibody specific for the C terminus of gp120. Serial dilutions of KD-247 or 447-52D were tested for binding by ELISA. Because of differences in the amount of bound gp120, optical density at 405 nm (OD_{405}) values were normalized to saturating levels of antibody (5 μg/ml) for comparison. Conc, concentration.

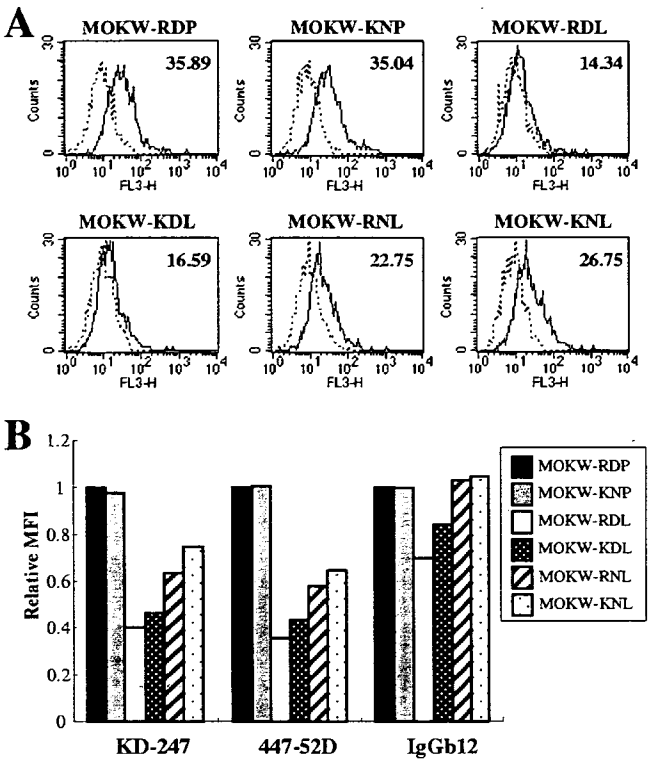

FIG. 8. Comparison of antibody binding to cell surface-expressed MOKW Env proteins with V2 mutations. (A) 293T cells transfected with MOKW Env-expression vectors were harvested at 24 h posttransfection and stained with KD-247. Flow cytometry data for binding of the KD-247 (black lines) to cell surface MOKW Env proteins are shown for GFP-gated 293T cells along with data for the control antibody (normal human IgG; dotted lines). The number at the top right of each graph is the MFI. (B) Each bar indicates relative binding of KD-247, 447-52D, and IgGb12 to MOKW Env-expressing cell surfaces. Data were normalized to each antibody's MFI for MOKW-RDP virus. FL3-H, relative fluorescence.

more prevalent than KN at positions 166 and 167 in the V2 region before selection (Fig. 2), the MOKW variants with 166K/167N/175L were selected and outgrown under KD-247 pressure (Fig. 2). It was possible that the KN sequences at positions 166 and 167 are necessary to compensate for the fitness of the variants with 175L in PM1/CCR5 cells, as shown in Fig. 6. To clarify the role of KN at positions 166 and 167 in replication, we constructed replication-competent viruses with a MOKW Env with RD or KN in addition to 175L (NL-MOKW-RDL and NL-MOKW-KNL) and compared their replication kinetics. As shown in Fig. 9, NL-MOKW-KNL virus replicated faster than NL-MOKW-RDL virus in PM1/CCR5 cells. These data suggested that KN sequences at positions 166 and 167 with the 175L variant confer a replication advantage in PM1/CCR5 cells. Therefore, the intermediate-resistant variant MOKW virus with the KNL sequence in the V2 region might replicate more rapidly than the highly resistant variant MOKW virus with RDL against KD-247 in the course of selection.

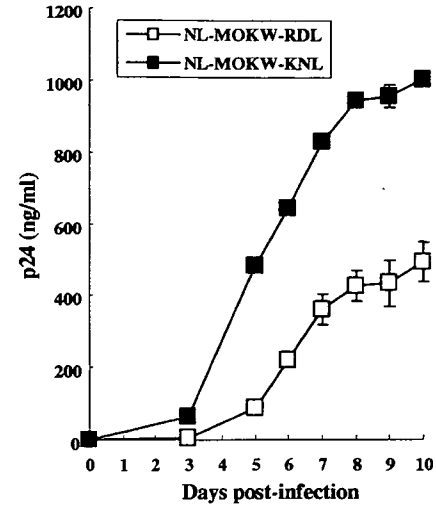

FIG. 9. Replication kinetics of infectious molecular clones NL-MOKW-RDL and NL-MOKW-KNL. PM1/CCR5 cells were exposed to NL-MOKW-RDL (open square) or NL-MOKW-KNL (filled square) and cultured for 10 days. Virus replication was monitored by measuring the amounts of p24 Gag protein produced in the culture supernatants. The data are representative of the results from two independent experiments.

DISCUSSION

Although an attack from the humoral immune response, especially anti-V3 NAb, is lasting against HIV-1 in vivo, it is not clear why the V3 tip sequence is conserved in the course of the infection. In the present study, by using a genetically heterogeneous HIV-1 primary R5 isolate, MOKW virus, we found that V2- and C3-mutated viruses expanded under conditions with a relatively low concentration of KD-247. Further, we found that the V3-tip-mutated virus was induced only under conditions with a high concentration of MAb (more than 500 μg/ml). Using region-swapping analysis, it was found that both V2 and V3 tip mutations can cause an escape phenotype against anti-V3 antibody. Neutralization escape variants with V2 mutations could be selected from quasi-species existing in the primary isolate at relatively low antibody pressures. On the other hand, highly resistant variants with amino acid substitutions in the V3 epitope emerged via evolution of the virus in the presence of a high concentration of the MAb.

The V1/V2 region of gp120 is highly diverse, not only in respect to virus subtypes but also in respect to intraspecies diversity in the same patient (16, 61, 66). The primary isolate, MOKW, also displayed diversity in the V2 region (Fig. 2), and the first-passaged virus already harbored mutations in the V2 region. Many researchers have reported that the V1/V2 domain strongly influences neutralization of the anti-V3 MAbs, MAbs to the other epitopes, and rsCD4 (12, 13, 25, 27, 30, 44, 49, 50). Moreover, structural models of the Env trimer have been proposed that place the base of the V1/V2 loop of one subunit in proximity to the V3 loop of a neighboring subunit (32, 34). In the present study we observed a reduction in the binding of anti-V3 MAbs to V2-mutated Env expressed on the cell surface, whereas mutations in V2 did not have an effect on the binding of the MAbs to monomeric gp120. These results suggest the association of V2 mutations with anti-V3 antibody